Hindawi
Journal of Advanced Transportation
Volume 2022, Article ID 8964170, 23 pages
https://doi.org/10.1155/2022/8964170

Research Article

Improved Driveway Design for Superblocks to Reduce the Crash Risk

Xi Zhuo,[1] **Panos D. Prevedouros**,[2] **Yongqiang Zhang**,[3] **Changtai Lu**,[1] **Yuxin Xiao**,[1] **and Weifan Zheng**[1]

[1]*College of Civil Engineering, Fuzhou University, Fuzhou 350108, China*
[2]*Department of Civil and Environmental Engineering, University of Hawaii at Manoa, Honolulu 96822, USA*
[3]*College of Automobile and Traffic Engineering, Nanjing Forestry University, Nanjing 210037, China*

Correspondence should be addressed to Panos D. Prevedouros; pdp@hawaii.edu

Received 21 June 2021; Revised 24 December 2021; Accepted 27 December 2021; Published 18 March 2022

Academic Editor: Yajie Zou

The superblock has become a typical land use in China and many growing Asian cities. Superblock access points generate traffic congestion and many conflicts among all road users. Driveway design is a critical process and has a major impact on traffic conditions around superblocks. There are various guidelines for the two key factors for driveway design, driveway width and curb radius, but they provide reference values corresponding to traffic volume and speed; these are not sufficient for managing the complex traffic environment around superblocks. To improve driveway design, we develop detailed access point design models that account for conflicts between turning and through motorized vehicles, conflicts between motorized and nonmotorized traffic, speed differential larger than 10 km/h, and lane encroachments of entering and exiting vehicles. The crash risk models evaluate and optimize the combination of driveway width and curb radius with respect to three traffic safety indexes: traffic conflict, lane encroachment, and speed differential. A case study evaluation shows that the updated driveway design models produce a lower crash risk; seven of the ten driveways improved by 16.14% or more. The updated driveway design for superblocks would be beneficial for analyzing, permitting, and managing traffic operations at superblocks and oversized development with many and complex driveways.

1. Introduction

Superblock is an urban area of several acres, usually closed to through traffic, having a mix of land uses including residential, commercial, social, and recreational facilities [1]. A typical block in Manhattan in New York City is about 80 m × 275 m (260 ft by 900 ft), and in Chicago, Illinois, and Minneapolis, Minnesota, a typical city block is 100 m × 200 m (330 ft by 660 ft). A superblock is much larger than a typical city block. For example, in New York City, the Stuyvesant Town private market and residential superblock take up about 18 city blocks. In China, the superblock measures about 300 m × 500 m [2]. The superblock has played an important role in the urban growth of China and other major cities in Asia. A superblock is characterized by dense land use that includes housing, businesses, and entertainment venues. Superblocks tend to generate heavy traffic on the adjacent streets; they tend to be congested and the traffic safety risk is elevated due to the multitude of users and maneuvers. Additionally, Ewing et al. have found that the more connected street networks have significantly lower congestion levels, but they do not have measurably lower (or higher) crash rates, presumably due to the prevalence of four-way intersections [3]. Consequently, it is meaningful for us to investigate the relationship between traffic safety and superblock design which plays an important role in street connectivity.

Access management strategies can help alleviate traffic problems at superblocks. Access management is the coordinated planning, regulation, and design of access between roadways and land development [4]. Many states in the US have developed access management guidelines, for example, Access Management Guidebook for Texas [5], Access

Management Guidebook for Michigan [6], and Access Management Regulations for Virginia [7]. They are focused on providing efficient and safe access for vehicles and pedestrians. They pay more attention to certain traffic management techniques, which are divided into two main parts. One part addresses access spacing, zoning, setbacks, and so on, and the other part addresses frontage roads, medians, turning control, access location, and driveway design [8].

The American Association of State Highway and Transportation Officials (AASHTO) provided a fundamental guidance for access management, which is applicable to superblock traffic management, but had limitations [9]. In response to these limitations, in 2019, the National Cooperative Highway Research Program (NCHRP) planned to award a contract for a study and report on “Public Liabilities Relating to Driveway Permits” [10]. Across the USA, there are approximately 2,000 driveway-related crashes per day with about 600 injuries. Therefore, in terms of driveway permits, there is a debate about balancing public interests (safety, efficiency) and private interests (profitability, convenience, and market value). Chakraborty and Gates analyzed safety impacts of driveways of various land utilization and found that commercial driveways possess a stronger effect on crash occurrence than other driveways of land use types, including residential and industrial driveways [11]. A more detailed and logical driveway design method which adapts more closely to the traffic environment of various land use would make the design and review of driveways easier, given that the stage of driveway permitting is critical to the approval and success of a superblock development. The superblock design presented herein also applies to extra-large urban block development and for theme parks, stadiums, and other large developments with multiple driveways.

Driveway design is mainly composed of methods to design length, width, median, cross slope, intersection angle, horizontal alignment, grade, and auxiliary lanes of driveways [12]. Compared with urban streets, driveway design has its distinct geometry, road environment, and traffic operations. The basic design parameters are shown in Figure 1; the driveway width provides adequate space for vehicles entering and leaving the superblock. The width of a driveway should reflect the needs of both motorized and nonmotorized traffic [12]. Various guidelines provide reference values for the driveway width based on traffic volume, design vehicles, design speed, and so on. However, for complex driveways such as those at superblocks and other large venues, it is meaningful to develop a model for driveway width, which is adaptive to a complex access environment, instead of a design that only satisfies a few fixed standards.

In Figure 1, the curb radius should assist right-turning vehicles with more smooth trajectories. A small radius causes a tight turn and may lead to encroachments of the curb or other lanes on the driveway or the main road [13]. To provide easier entry and exit movements for vehicles, guides give reference values of the curb radius, depending on the volume and speed of vehicles.

Driveway width and curb radius are interrelated. If the curb radius is short, the vehicle needs a longer width to complete the entry movement, as shown in Figure 2 [4].

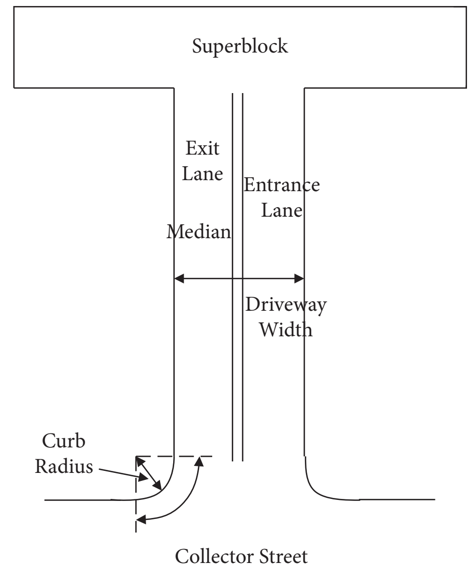

Figure 1: Width and curb radius of the driveway.

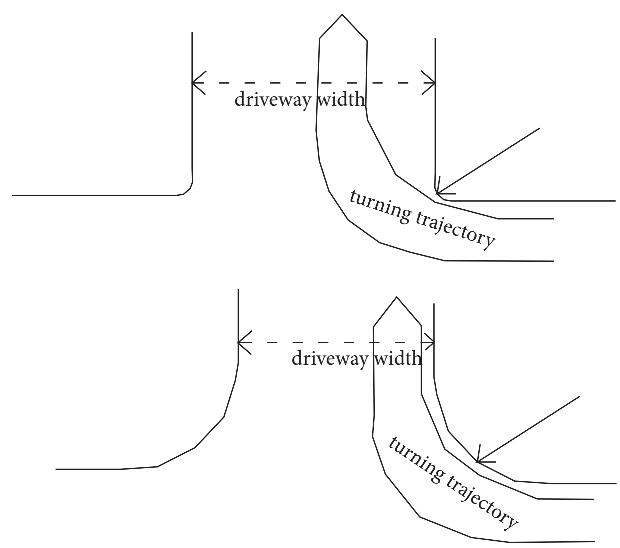

Figure 2: Turning trajectory of entry maneuver.

NCHRP Report 659 provides reference values of combination of driveway width and curb radius, corresponding to a driveway entry speed [12]. The recommended values may not suit the whole range of access management and superblock access in particular. A quantitative model for the joint estimation of driveway width and curb radius is needed. Zou et al. applied the Bayesian Model Averaging for analyzing freeway traffic incident clearance time for emergency management, which can be used for predicting traffic incident clearance time when model uncertainty is considered [14]. The method provides the theory basis for optimizing the combination of driveway width and curb radius to reduce the crash risk.

The remainder of this paper is organized as follows. In Section 2, we present past studies related to our research, including studies about superblock traffic management, the relationship between the driveway width and curb radius, and evaluation methods for driveway design. In Section 3, we present driveway width models based on conflicts between turning and through vehicles and those between motorized and nonmotorized traffic. In Section 4, we propose curb radius models, which consider entering and exiting turns, aiming at reducing the phenomenon of larger speed differential between turning and through vehicles, and lane encroachment. In Section 5, we present crash risk models to evaluate and optimize the combination of driveway width and curb radius by analyzing number of traffic conflicts. In Section 6, we conduct a case study on a superblock in China to evaluate the developed models. In Section 7, we discuss the pros, cons, and use value of the models. In Section 8, we present the conclusions of our study.

2. Past Research and Guidance

The superblock concept establishes a hierarchy of surrounding streets by separating through roads and roads serving local traffic [15]. The driveway is the connection between the Superblock Collector Street adjacent to the superblock and internal roads of the superblock. Throughout this paper, we use SCS for Superblock Collector Street to represent the roadway adjacent to the superblock. These connections often become bottlenecks due to the large number of turning movements and interference with pedestrians and nonmotorized traffic. Therefore, the design of driveways is a critical component of a superblock.

AASHTO's Green Book includes driveway width guidelines, which provide reference values of driveway width and number of lanes based on driveway usage [9]. NCHRP Report 659 indicates that design vehicle and design speed are fundamental factors affecting the driveway width design, and the width of a driveway is a function of the number of driveway lanes, the width of those lanes, and the presence and width of the median, if applicable [12].

Levinson et al. state that the elements of driveway entry width (throat width), entry geometry (curved radius or straight taper), and entry shape dimensions must be considered together [16]. NCHRP Report 659 points out that the driveway width and the curb radius can perform in concert, so to some degree one can increase as the other decreases, which means that if the entry speed is constant, then there is an inverse relationship between entry radius and entry lane width [12]. An FHWA synthesis shows the relationships between driveway width, curb radius, and vehicle speed [17]. The Access Management Manual suggests that a designer could choose from a number of combinations of driveway width and curb radius, taking the design speed and driveway use intensity into account, and it is possible that the choice of minimum and maximum radii from one table and the minimum and maximum driveway widths from another table may cause conflicts in design [4]. Stover and Koepke found that a better practice is to use a specific combination of radius and throat width to accommodate a selected design condition [18], and NCHRP Report 15–35 indicates that certain collision types on the driveway, such as rear-end, right-angle, and head-on angle, are caused by the maneuvers of entering and exiting vehicles, which yields the fundamental safety or conflict points to optimize the combination of width and radius [19]. It is interesting that some researchers found that increasing the driveway width increases the crash frequency, but increasing the number of driveway entry lanes from 1 to 2 decreases the crash rate [20].

Sultana et al. used a generalized negative binomial model to identify the impact of access parameters on truck-related crashes [21]. Their study demonstrated that significant factors in crash frequency prediction include standard deviation of commercial driveway throat width, flared commercial driveway throat width and its standard deviation, proportion of divided commercial driveways, signal density, and shoulder width. Chowdhury et al. evaluated different kinds of driveway design; each of the access management alternatives was evaluated in terms of travel time, number of stops, delay, and stopped delay using microscopic traffic simulation [22]. They found that the effectiveness of access management strategies is site-specific, but the driveway consolidation strategy yields a consistent improvement on almost all study corridors in terms of travel time. Richards studied the effects of driveway width, curb radius, and offset taper approach treatments on the speed and path of driveway users; his study found that average entry speed decreased as available width and/or curb radius decreased, and if the curb radius is large, then the path of vehicles turning right into the driveway tended to parallel the entry curb line [23].

The aforementioned literature suggests that driveway design is important for access. The various guides focus mostly on reference values and qualitative guidelines of driveway width and curb radius. Our proposed driveway model includes width and curb radius, is based on spatiotemporal vehicle paths on the driveway and the adjacent street, and facilitates analysis with simulation and regression methods.

3. Driveway Width Models

To reduce conflicts, we propose models of driveway width and then combine them to find a better estimate for width. There are two types of typical entering movements, that is, 2 and 3 in Figure 3, and two types of typical exiting movements, that is, 1 and 4 in Figure 3. Driveway width influences the possibility of exiting vehicles to use the gap in the through traffic flow, while it does not affect entering turns directly. Therefore, our research focuses on exiting movements 1 and 4 in Figure 3.

For exiting movements, there are two types of crossing conflict areas. One is the conflict area of the motorized traffic; the other is the conflict area between the motorized and nonmotorized traffic.

3.1. Conflicts between Left-Turning and through Vehicles. Normally, the SCS is a two-way street. If there is no median on the SCS, left-turning vehicles would cross the through traffic flow, as shown in Figure 4.

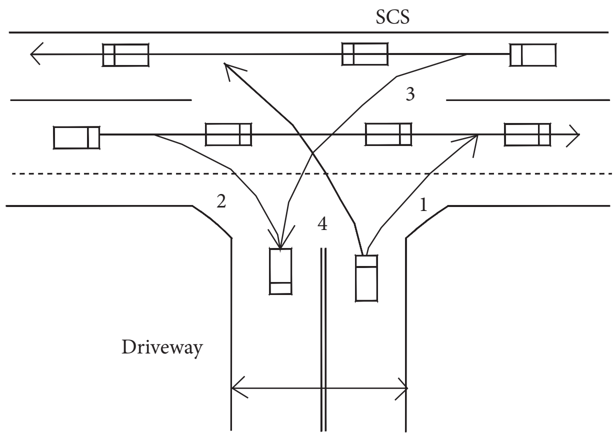

Figure 3: Typical movements between SCS and driveway.

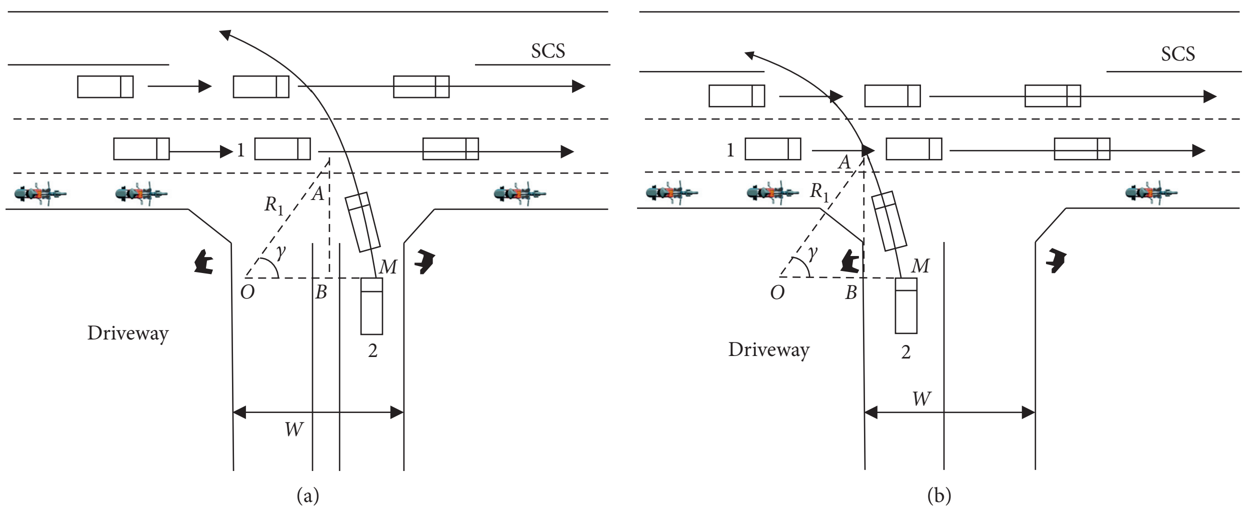

Figure 4: Left-turning on two-way SCS. (a) Right-side left-turning. (b) Left-side left-turning.

Sometimes, the SCS is a one-way street, so an exiting vehicle should turn left to merge into the traffic flow, as shown in Figure 5.

Figures 4 and 5 have similar traffic features, so we consider them together. There is a crossing conflict between left-turning vehicle 2 on the exit lane and through vehicle 1 on the SCS (see Figure 5). In this study, we make the following assumptions:

(1) Vehicle 1 is on the lane nearest to the superblock access.

(2) Trajectory of turning vehicle 2 is a circular arc.

(3) Vehicle 2 keeps the same turning radius for the whole turn.

(4) Point M, the starting point of turning trajectory, is in the middle of the exit lane on the driveway.

(5) Point A is the position of the front of vehicle 2 at the boundary of conflict area. When vehicle 2 turns left, A is on the extended centerline or the edge line of the driveway. Point B is the point of intersection between line OM and vertical line through point A. Point O is the center of turning circle. ΔABO is a right-angled triangle, which implies that OM is perpendicular to the driveway centerline or edge line.

(6) The widths of entrance and exit lanes are the same.

The minimum gap that all drivers in the minor stream are assumed to accept at all similar locations is the critical gap t_c (s) [24]. So t_{cl} (s) is the minimum gap for left-turning vehicle 2 to leave the driveway and pass over the conflict area, shown in the following equation:

$$t_e + t_2 \geq t_{cl}, \tag{1}$$

where t_e is the travel time for vehicle 2 to enter the boundary of the conflict area(s); t_2 is the time for vehicle 2 to pass through the conflict area(s).

In Figure 5, by analyzing the geometrical relationship in this crossing conflict, we find that t_e could be calculated by the following formula:

$$t_e = 3.6 \arccos\left(\frac{R_l - W/4}{R_l}\right)\frac{R_l}{V_{ae}}, \tag{2}$$

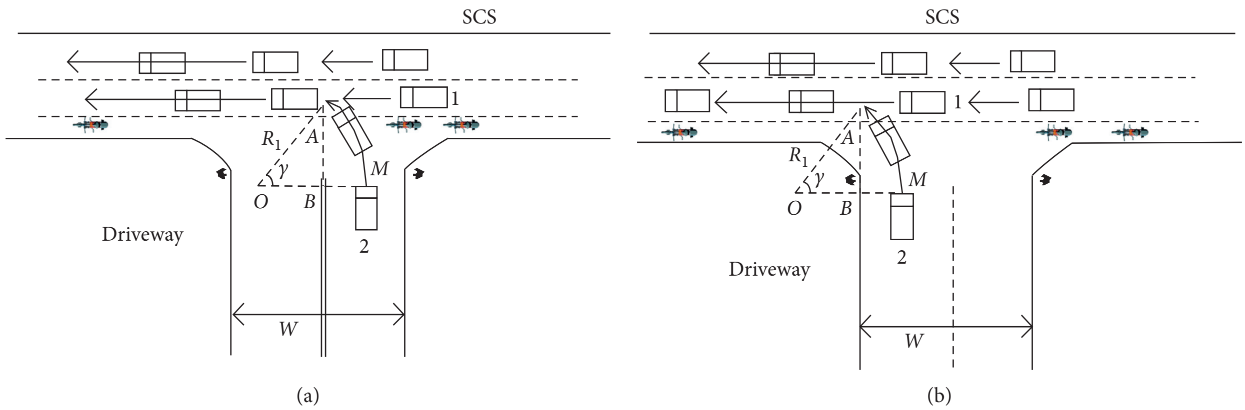

FIGURE 5: Left-turning on one-way SCS. (a) Right-side left-turning. (b) Left-side left-turning.

where R_l is the radius of left-turning trajectory (m); W is the width of driveway (m); V_{ae} is the average travel speed of vehicle 2 (km/h).

Then as the adequate driveway width is beneficial for vehicle 2 to cross the conflict area formed by the conflict between vehicle 1 and 2, we have the equations below.

t_2 can be calculated by the following equation:

$$t_2 = \frac{3.6W_{veh}}{V_{ae}}, \tag{3}$$

where W_{veh} is the width of vehicle (m).

Combining equations (1)–(3), we can calculate W by using the following equation:

$$W \le 4R_l - 4R_l \cos\left(\frac{V_{ae}t_{cl} - 3.6W_{veh}}{3.6R_l}\right). \tag{4}$$

3.2. Conflicts between Right-Turning and through Vehicles. When vehicle 2 turns right from the driveway to the SCS, vehicle 2 should merge into the traffic flow of the lane nearest to the superblock on the SCS (see Figure 6). In addition to the assumptions above, we also assume that when vehicle 2 turns right, A is on the centerline of the lane nearest to the superblock on the SCS.

We also get the following formula to present the relationship between travel time and gap:

$$t_e + t_3 \ge t_{cr}, \tag{5}$$

where t_3 is the time for vehicle 2 to turn right into the through traffic flow(s); t_{cr} (s) is the minimum gap for right-turning vehicle 2 to leave the driveway and merge into the through traffic flow.

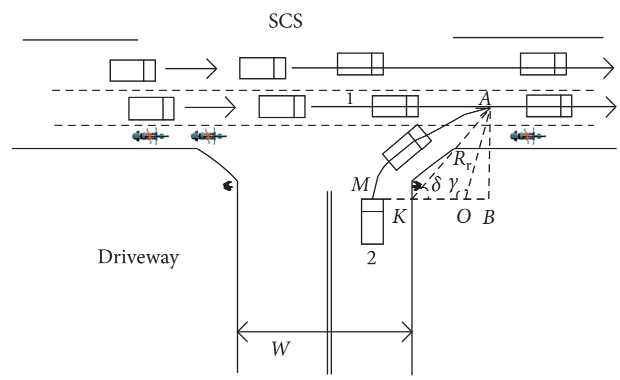

FIGURE 6: Conflict between right-turning and through vehicles.

In Figure 6, point K is the point of intersection between line BM and the edge line of driveway. Further, according to the law of cosines, we derive the following formula for the angle at the center of arc $\overset{\frown}{AM}$, that is, γ (rad):

$$\begin{aligned}\gamma &= \arccos\left(\frac{KO^2 + AO^2 - AK^2}{2KO \times AO}\right) \\ &= \arccos\left[\frac{(R_r - W/4)^2 + R_r^2 - (W_{cro} + W_{nv} + W_{lu}/2)^2/\sin^2\delta}{2(R_r - W/4)R_r}\right],\end{aligned} \tag{6}$$

where KO is the distance of line KO (m); AO is the distance of line AO (m); AK is the distance of line AK (m); R_r is the radius of right-turning trajectory (m); W_{cro} is the width of crosswalk (m); W_{nv} is the width of nonmotorized vehicle lane (m); W_{lu} is the width of the lane nearest to the superblock on the SCS (m); δ is the included angle between line AK and line BK (rad).

Therefore, with equation (6), we find that t_e can be calculated as follows:

$$t_e = \frac{3.6\gamma R_r}{V_{ae}} = 3.6 \arccos\left[\frac{(R_r - W/4)^2 + R_r^2 - (W_{cro} + W_{nv} + W_{lu}/2)^2/\sin^2\delta}{2(R_r - W/4)R_r}\right]\frac{R_r}{V_{ae}}. \quad (7)$$

t_3 is

$$t_3 = \frac{3.6W_{veh}}{V_{ae}}. \quad (8)$$

Combining equations (5), (7), and (8), we calculate W as follows:

$$3.6 \arccos\left[\frac{(R_r - W/4)^2 + R_r^2 - (W_{cro} + W_{nv} + W_{lu}/2)^2/\sin^2\delta}{2(R_r - W/4)R_r}\right]\frac{R_r}{V_{ae}} + \frac{3.6W_{veh}}{V_{ae}} \geq t_{cr}. \quad (9)$$

3.3. Conflicts between Motorized and Nonmotorized Traffic. When the vehicle turns left or right, the motorized and nonmotorized traffic have to share the same space on the crosswalk, as there are normally no pedestrian signals at the driveway.

The nonmotorized traffic is able to safely traverse the driveway, only if the time gap between arrivals of the motorized and nonmotorized traffic is greater than the threshold for the crossing decision of the nonmotorized vehicle t_{mn} (s) or the decision standard of pedestrian t_{vp} (s) [25], as shown in Figure 7.

(1) Considering the conflict area between motorized and nonmotorized vehicles, we propose the following equation:

$$\left(\frac{3.6l_m}{V_{ae}}\right) - \left(\frac{3.6l_{nm}}{V_{nm}}\right) \geq t_{mn}, \quad (10)$$

where l_m is the distance from the head of the exiting vehicle to the collision point between motorized and nonmotorized vehicles (m); l_{nm} is the distance from the location of a nonmotorized vehicle beginnig to move to the edge of conflict area(m); V_{nm} is the velocity of nonmotorized vehicle (km/h).

Considering the safety distance between motorized and nonmotorized vehicles, we assume that l_{nm} is equal to the half of the driveway width W. Therefore, based on equation (10), W can be calculated as follows:

$$W \leq 2\left(\frac{l_m V_{nm}}{V_{ae}}\right) - \left(\frac{t_{mn}V_{nm}}{1.8}\right). \quad (11)$$

Stopping sight distance is needed to check the road visibility, so that drivers can identify the dangerous object and control the vehicle to stop safely in front of it. When the vehicle exits, the driver requires adequate time to identify and deal with the possible collision point, so the distance from the head of the exiting vehicle to the collision point between motorized and nonmotorized vehicles l_m must be long enough to ensure that the driver can see, understand, and react to the collision point in the crosswalk and then stop the car. Consequently, the distance l_m longer than stopping sight distance may be meaningful. Therefore, we assume that the minimum value of l_m is the sum of the stopping sight distance [26] and the width of crosswalk.

$$l_{m,min} = \frac{V_{dd}t_{pr}}{3.6} + \frac{V_{dd}^2}{254(\varphi + i')} + l_0 + W_{cro}, \quad (12)$$

where $l_{m,min}$ is the minimum value of l_m (m); V_{dd} is the design speed of driveway (km/h); t_{pr} is the perception-reaction time (s); φ is the longitudinal friction coefficient between the vehicle and the pavement; i' is the driveway slope; l_0 is the safety space headway (m).

Superblock has very limited land resources, which are compact and valuable. If the driveway width is too large, there would be less land for development in superblocks. Therefore, we think that, on the basis of meeting the requirement of traffic safety, the smaller driveway width means the better land use efficiency for superblocks. Furtherly, according to equation

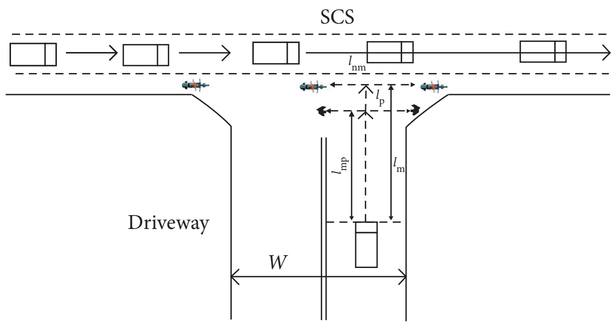

Figure 7: Crossing decision process.

(11), smaller value of l_m would lead to smaller W alternative values, which can still meet the demand of traffic safety. Therefore, with equation (11), we use $l_{m,min}$ to obtain the possible W alternative values, which has both advantages of avoiding conflicts between motorized and nonmotorized vehicles and promoting efficient use of land resources for superblocks as follows:

$$W \leq 2\left(\frac{l_{m,min} V_{nm}}{V_{ae}}\right) - \frac{t_{mn} V_{nm}}{1.8}. \qquad (13)$$

Combining equations (12) and (13), we find the following model:

$$W \leq 2\left[\frac{V_{dd} t_{pr}}{3.6} + \frac{V_{dd}^2}{254(\varphi + i')} + l_0 + W_{cro}\right] \frac{V_{nm}}{V_{ae}} - \frac{t_{mn} V_{nm}}{1.8}. \qquad (14)$$

(2) For the conflict area between vehicles and pedestrians, there is the following equation [25]:

$$\frac{3.6 l_{mp}}{V_{ae}} - \left(\frac{3.6 l_p}{V_p}\right) \geq t_{vp}, \qquad (15)$$

where l_{mp} is the distance from exiting vehicle head to the position that vehicle rear is at the edge of crosswalk (m); l_p is the distance from the location of a pedestrian to the edge of conflict area (m); V_p is the velocity of a pedestrian (km/h).

We assume that l_p is equal to one half of the driveway width. Based on equation (15), W can be calculated as follows:

$$W \leq 2\left(\frac{l_{mp} V_p}{V_{ae}}\right) - \frac{t_{vp} V_p}{1.8}. \qquad (16)$$

Similarly as mentioned above, we assume that the minimum value of l_{mp} is the stopping sight distance [26], and then, according to equation (16), W is calculated as follows:

$$W \leq 2\left[\frac{V_{dd} t_{pr}}{3.6} + \frac{V_{dd}^2}{254(\varphi + i')} + l_0\right] \frac{V_p}{V_{ae}} - \frac{V_p t_{vp}}{1.8}. \qquad (17)$$

4. Curb Radius Models

Adequate curb radius would help a turning vehicle travel faster, reducing the speed differential between the turning and through vehicles, and would keep it from encroaching the adjacent lane. To achieve these two goals, we propose models of curb radius.

For right turns, there are four possible combinations of turning movements, as shown in Figure 8.

For left turns, there are also four turning combinations, as shown in Figure 9.

From Figures 8 and 9, we observe that trajectories of turning movements 1 and 2 are at the near side of the curb, so curb radius affects and guides the movements. However, as turning movements 3 and 4 are at the far side of the curb, the curb radius cannot affect them directly. It can be found that, for a small curb radius, movement 1 or 2 may affect movement 4 or 3, as shown in Figure 10. In other words, the impact of curb radius on movement 1 or 2 is a critical factor for curb radius models.

Our research focuses on movements 1 and 2 in Figures 8 and 9, with the following assumptions:

(1) The starting point of travel trajectory of turning vehicle is at the edge of the curb

(2) The trajectory of turning vehicle is a curve, defined by a composite function (e.g., equation (18) or (32) [27])

(3) Turning vehicles travel between the lane nearest to the superblock on the SCS and the driveway

As the entering and exiting turning trajectories have different traffic impacts, the curb radius models are different.

4.1. Radius Based on Entering Turns. We analyze the entering right-turn trajectories, with respect to different types of radius, as shown in Figure 11.

Vehicles turn left from the one-way SCS into the superblock, as shown in Figure 12.

As Figures 11 and 12 have similar traffic features, we consider them together. For the turning trajectory, a coordinate system is put forward, where vertical line through the starting point of turning trajectory is the x-axis, and the edge line of the lane nearest to the superblock on the SCS is the y-axis. We assume that, in this coordinate system, the turning vehicle decelerates slowly from point C, the starting point of vehicle trajectory, to point D, the effective starting point of turning movement, and then turns to point H, the effective end point of turning movement, and accelerates to point E, the end point of vehicle trajectory. Point G is the point of intersection between driveway edge line and perpendicular line through point E, and point F is the point of intersection between perpendicular line through point D and line EG. CD and HE are straight lines, and DH is a curve of equation (18) [27].

Qu et al. gave models for indicating the right-turning vehicle trajectories at the signalized intersection [27]. When

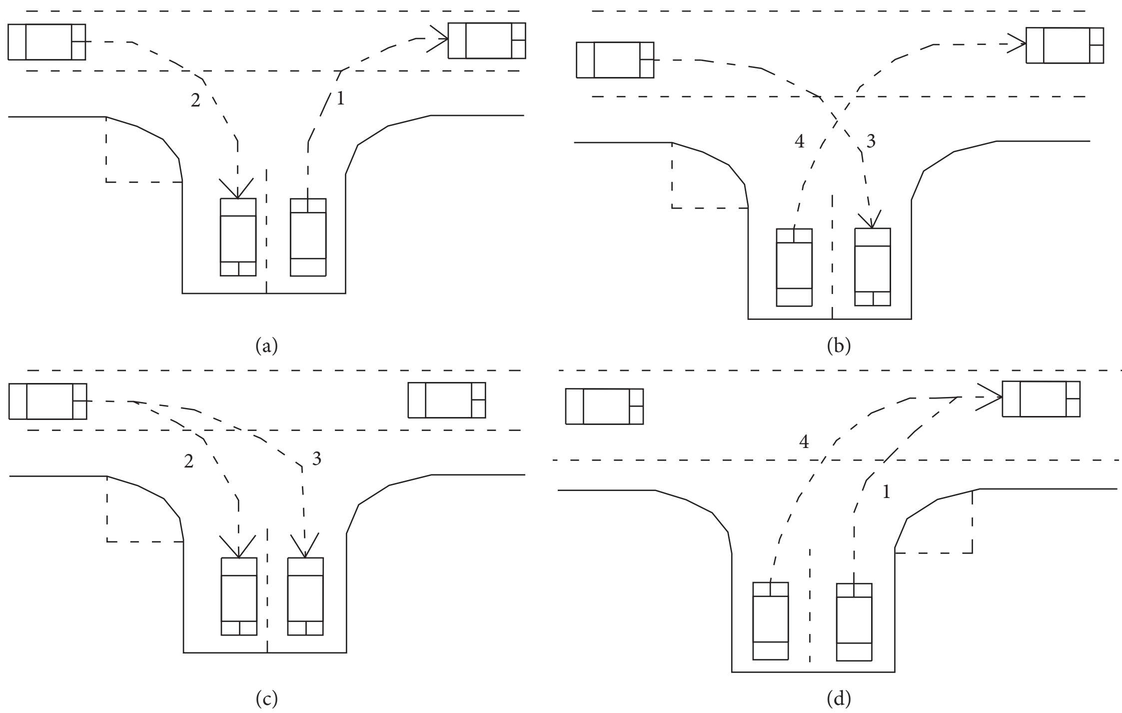

Figure 8: Combinations of right-turning movements. (a) Entering and exiting turns at the near side of the curb. (b) Entering and exiting turns at the far side of the curb. (c) Entering turns at the near and far side of the curb. (d) Exiting turns at the near and far side of the curb.

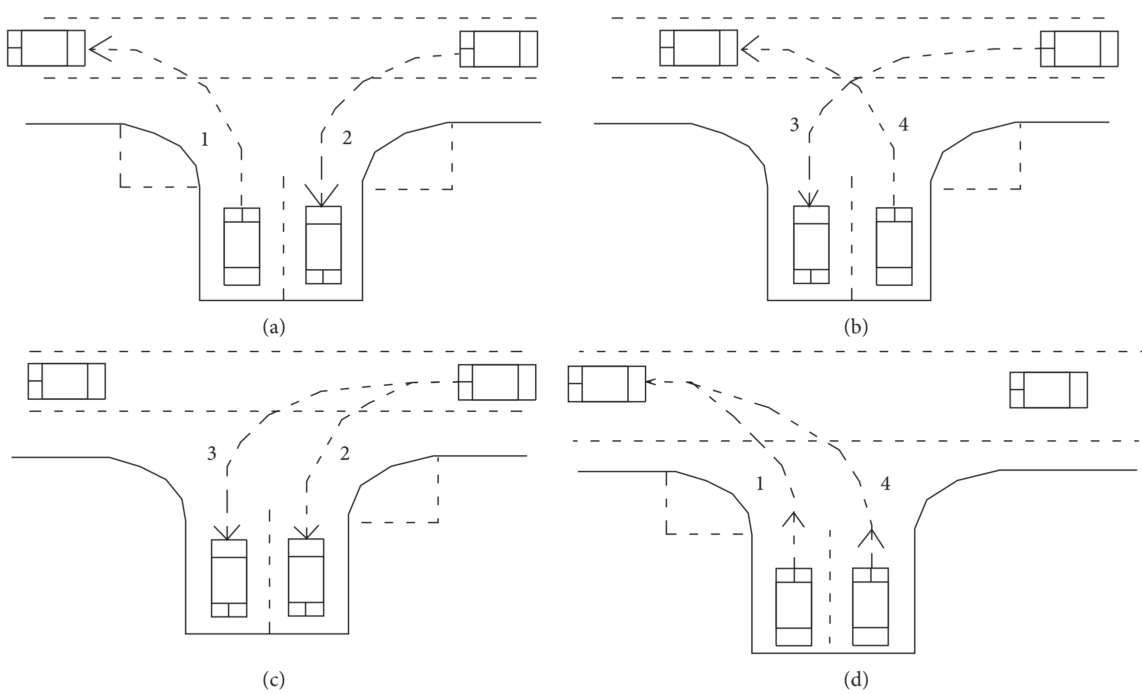

Figure 9: Combinations of left-turning movements. (a) Entering and exiting turns at the near side of the curb. (b) Entering and exiting turns at the far side of the curb. (c) Entering turns at the near and far side of the curb. (d) Exiting turns at the near and far side of the curb.

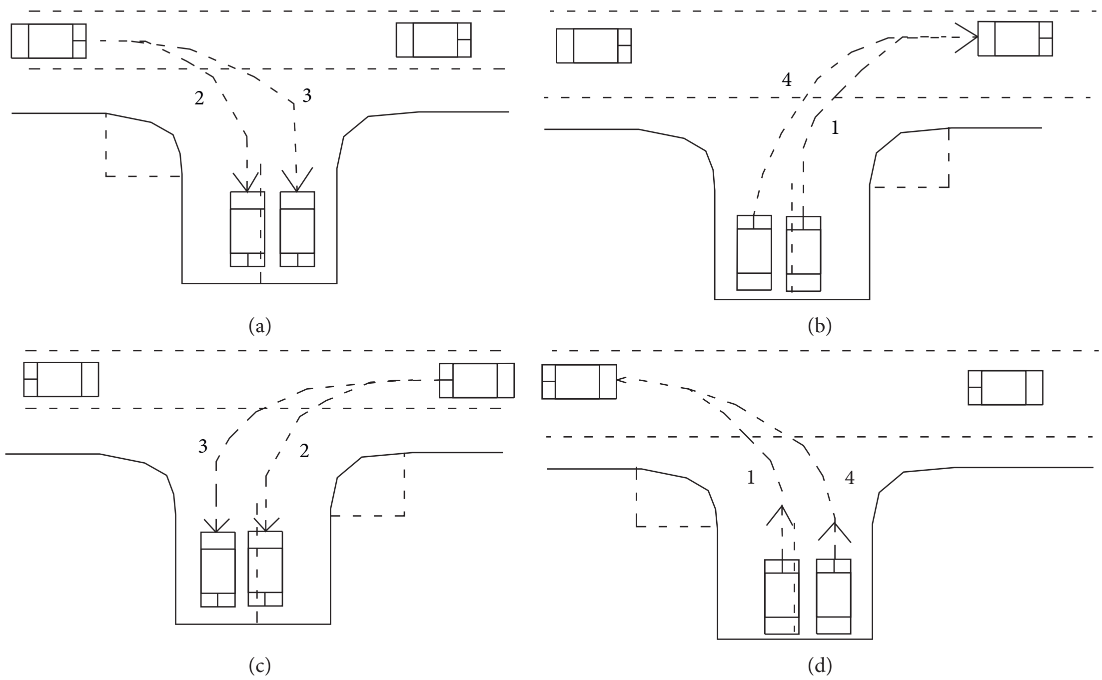

Figure 10: Interaction of turning movements. (a) Interaction of entering right turns. (b) Interaction of exiting right turns. (c) Interaction of entering left turns. (d) Interaction of exiting left turns.

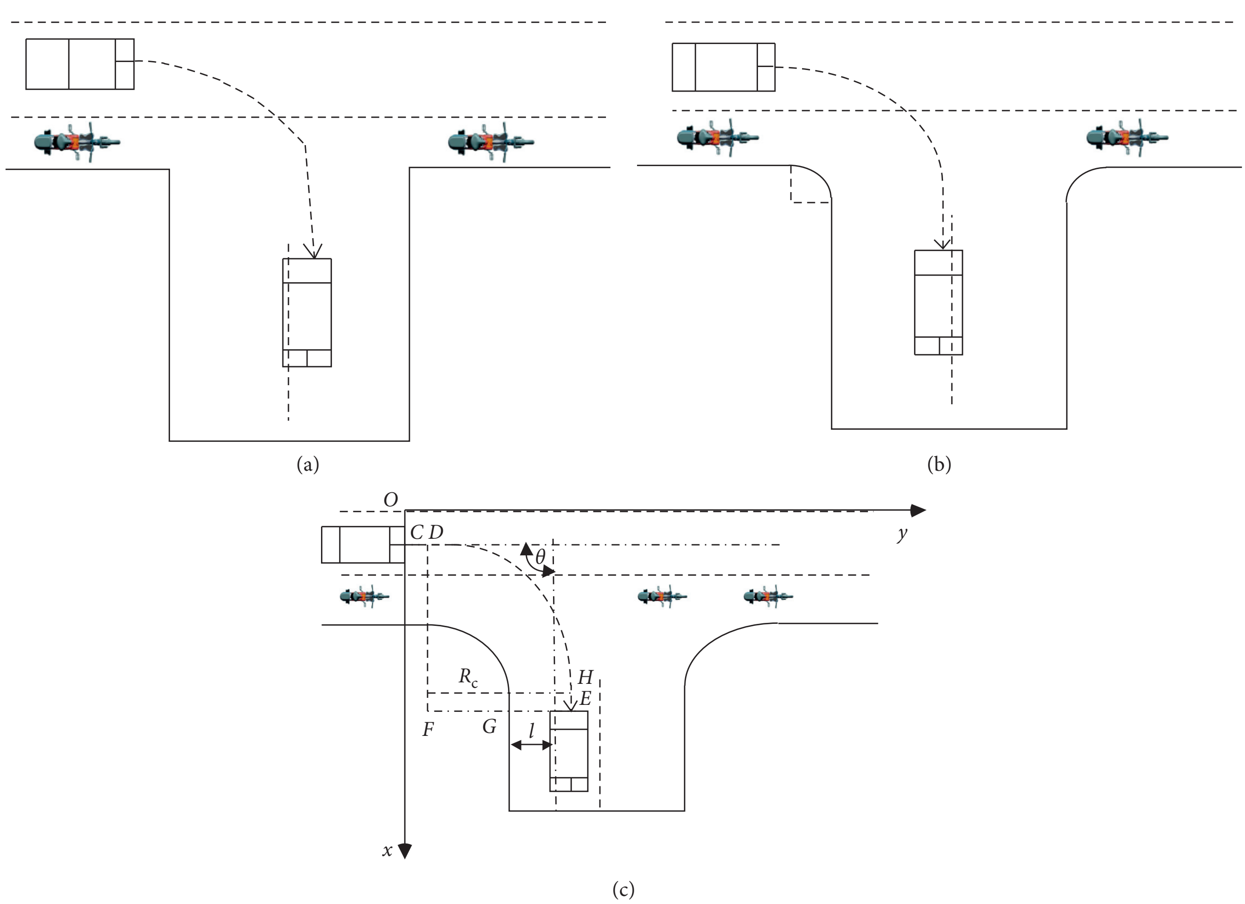

Figure 11: Right turns on the driveway. (a) Driveway without entering radius. (b) Driveway with small entering radius. (c) Driveway with large entering radius.

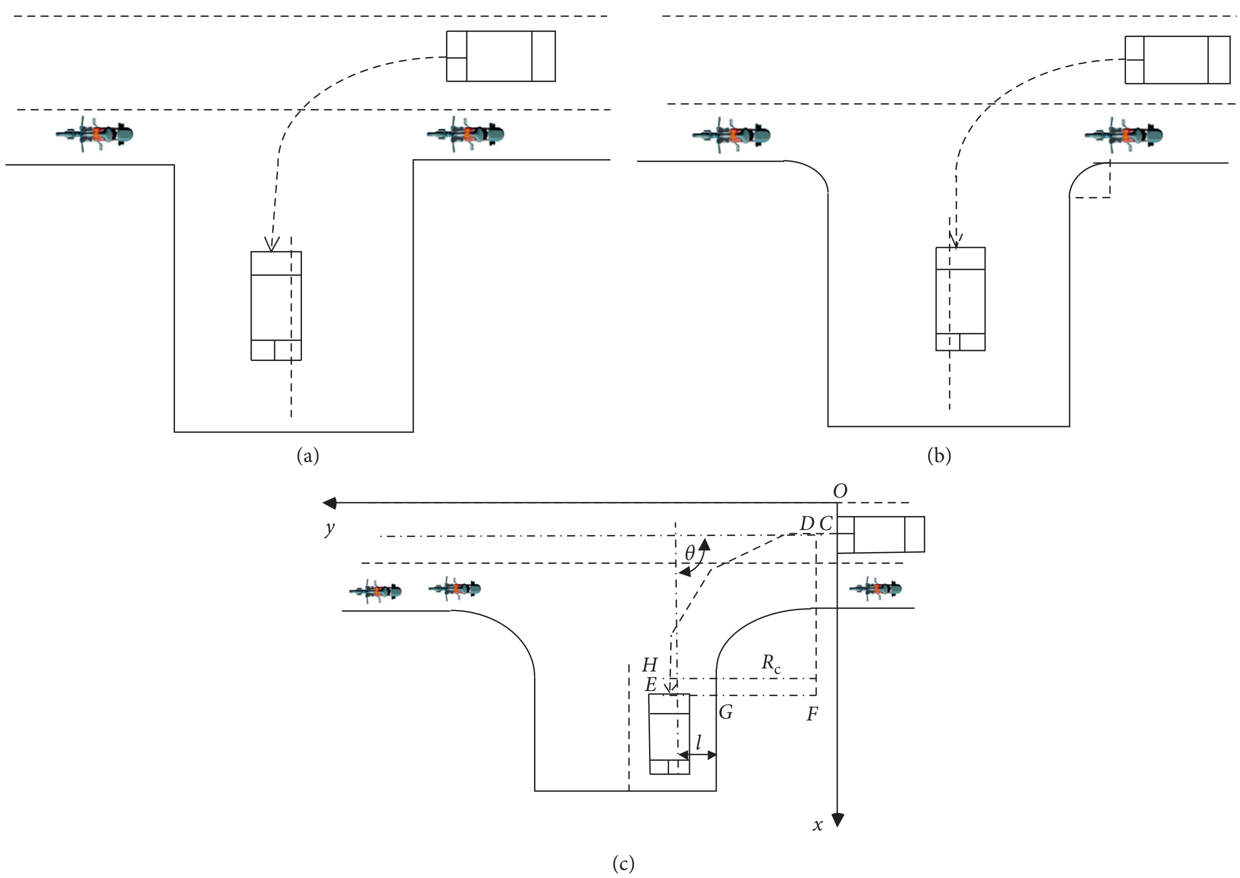

Figure 12: Left turns on the driveway. (a) Driveway without entering radius. (b) Driveway with small entering radius. (c) Driveway with large entering radius.

entering turns are hindered by the crossing nonmotorized traffic, which is exactly the problem depicted in Figures 11 and 12, their models [27] can be used as follows:

$$y = a + b \ln x + c\left(\frac{V}{3.6}\right)^2 + \frac{dV}{3.6}, \quad (18)$$

$$a = 20.453 - 0.699R_cN - 5.131l + 2.24R_c^2 + 1.314l^2, \quad (19)$$

$$b = 58.789 - 0.3472R_cN - 11.04l + 0.127R_c^2 - 10.599\theta^2, \quad (20)$$

$$c = 0.0721 + 0.039R_c - 0.417lN + 0.023R_c^2, \quad (21)$$

$$d = 153.9 - 1.623R_c - 208.2\theta - 1.325R_c^2 + 59.98\theta^2 + 3.985R_c\theta, \quad (22)$$

where y is the value of y-axis (m); x is the value of x-axis (m); a, b, c, and d are coefficients; V is the speed of turning vehicle (km/h); R_c is the curb radius (m); N is the number of traffic conflicts between turning vehicles and nonmotorized vehicles in the peak hour (h^{-1}); l is the distance between the centerline of the exit lane and the curb edge (m); θ is the angle of corner (rad).

It is the fact that driveways are normally perpendicular to SCS; that is, $\theta = \pi/2$. Considering the definition, l should be one quarter of driveway width W. Then, based on the models above, we propose a revised method for calculating the curb radius as follows:

(1) Lane encroachment: The objective of the method is to ensure that the turning vehicle would not encroach onto the adjacent lane, shown in the following equation:

$$\text{EG} - l + \frac{W_{\text{veh}}}{2} = \frac{W}{4}, \quad (23)$$

where EG is the distance between points E and G (m).

By analyzing the geometrical relationship and using equation (18), the following can be deduced:

$$\begin{aligned} EG &= EF - FG \\ &= y_E - y_F - R_c \\ &= y_E - y_D - R_c \\ &= \left(b \ln x_E + \frac{cV_E^2}{3.6^2} + \frac{dV_E}{3.6}\right) \\ &\quad - \left(b \ln x_D + \frac{cV_D^2}{3.6^2} + \frac{dV_D}{3.6}\right) - R_c, \end{aligned} \tag{24}$$

where EF is the distance between points E and F (m); FG is the distance between points F and G (m); y_E is the value of y-axis at point E (m); y_F is the value of y-axis at point F (m); y_D is the value of y-axis at point D (m); x_E is the value of x-axis at point E (m); V_E is the speed of turning vehicle at point E (km/h); x_D is the value of x-axis at point D (m); V_D is the speed of turning vehicle at point D (km/h).

(2) Speed differential: According to the People's Republic of China Industry Standard, that is, "Specifications for Highway Safety Audit" [28], the speed differential between neighboring road sections should be no more than 10 km/h:

$$V_D \geq V_C - 10, \tag{25}$$

where V_C is the speed of turning vehicle at point C (km/h).

Meanwhile, we assume that V_C is the same as the design speed of SCS V_{du} (km/h), and V_E is the same as the design speed of driveway V_{dd} (km/h).

(3) Location analysis: From Figures 11 and 12, we observe that x_D is one half of the width of the lane nearest to the superblock on the SCS W_{lu}. Additionally, by analyzing the geometrical relationship, x_E can be calculated as follows:

$$\begin{aligned} x_E &= x_H + HE \\ &= R_c + W_{lu} + W_{nv} + HE, \end{aligned} \tag{26}$$

where x_H is the value of x-axis at point H (m); HE is the distance between points H and E (m).

Qu et al. found that, during the right-turning process, the velocity of vehicles normally decreases and then increases [27]. So we assume that vehicle movement from point H to point E is as follows:

$$HE = \frac{V_E^2 - V_H^2}{2 \times 3.6^2 a_{EH}}, \tag{27}$$

where V_H is the speed of turning vehicle at point H (km/h); a_{EH} is the acceleration rate on the line between points E and H (m/s^2).

In accordance with assumption and analysis above, combining equations (18) to (27), we obtain the following formulas for R_c:

$$\begin{aligned} \frac{W}{2} - \frac{W_{veh}}{2} \leq \Bigg[& b \ln\left(R_c + W_{lu} + W_{nv} + \frac{V_{dd}^2 - V_H^2}{2 \times 3.6^2 a_{EH}}\right) + \frac{cV_{dd}^2}{3.6^2} + \frac{dV_{dd}}{3.6}\Bigg] \\ & - \left[b \ln\left(\frac{W_{lu}}{2}\right) + \frac{c\left(V_{du} - 10\right)^2}{3.6^2} + \frac{d\left(V_{du} - 10\right)}{3.6}\right] \\ & - R_c, \end{aligned} \tag{28}$$

$$b = 32.637 - 0.3472R_cN - 2.76W + 0.127R_c^2, \tag{29}$$

$$c = 0.0721 + 0.039R_c - 0.1043WN + 0.023R_c^2, \tag{30}$$

$$d = 4.637R_c - 1.325R_c^2 - 25.145. \tag{31}$$

4.2. Radius Based on Exiting Turns. We analyze the exiting right-turn trajectories, with respect to different types of radius, as shown in Figure 13.

Vehicles turn left from the superblock onto the one-way SCS, as shown in Figure 14.

As Figures 13 and 14 have similar traffic features, we consider them together. When exiting turns are also hindered by the crossing nonmotorized traffic in Figures 13 and 14, other models given by Qu et al. [27] can be used for these turning trajectories as follows:

$$y = a' + b' \ln x + c'\left(\frac{V}{3.6}\right)^2 + \frac{d'V}{3.6}, \tag{32}$$

$$a' = 19.986 - 0.892R_cN - 6.141l + 2.27R_c^2 + 1.213l^2, \tag{33}$$

$$b' = 61.134 - 0.3997R_cN - 11.431l + 0.1354R_c^2 - 11.58\theta^2, \tag{34}$$

$$c' = 0.0923 + 0.086R_c - 0.412lN + 0.012R_c^2, \tag{35}$$

$$\begin{aligned} d' = & 123.5 - 1.785R_c - 195.2\theta - 1.123R_c^2 + 52.34\theta^2 \\ & + 2.546R_c\theta, \end{aligned} \tag{36}$$

where a', b', c', and d' are coefficients.

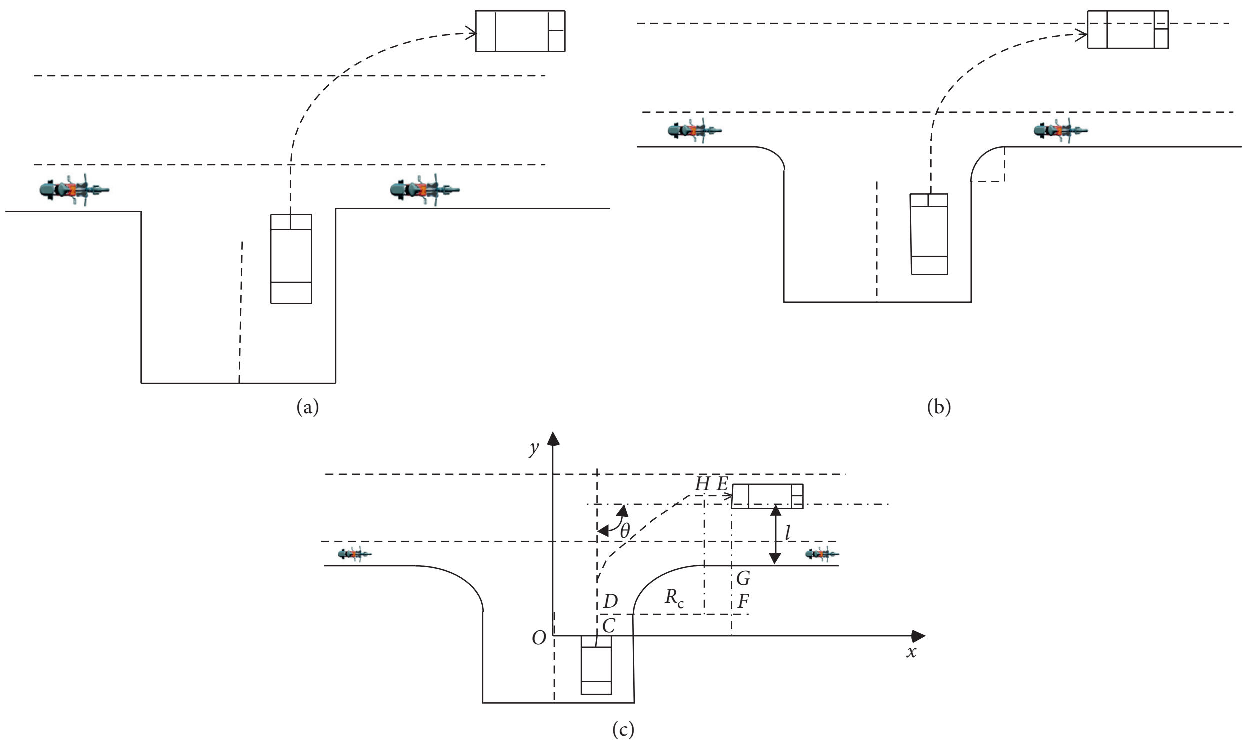

Figure 13: Right turns on the driveway. (a) Driveway without exiting radius. (b) Driveway with small exiting radius. (c) Driveway with large exiting radius.

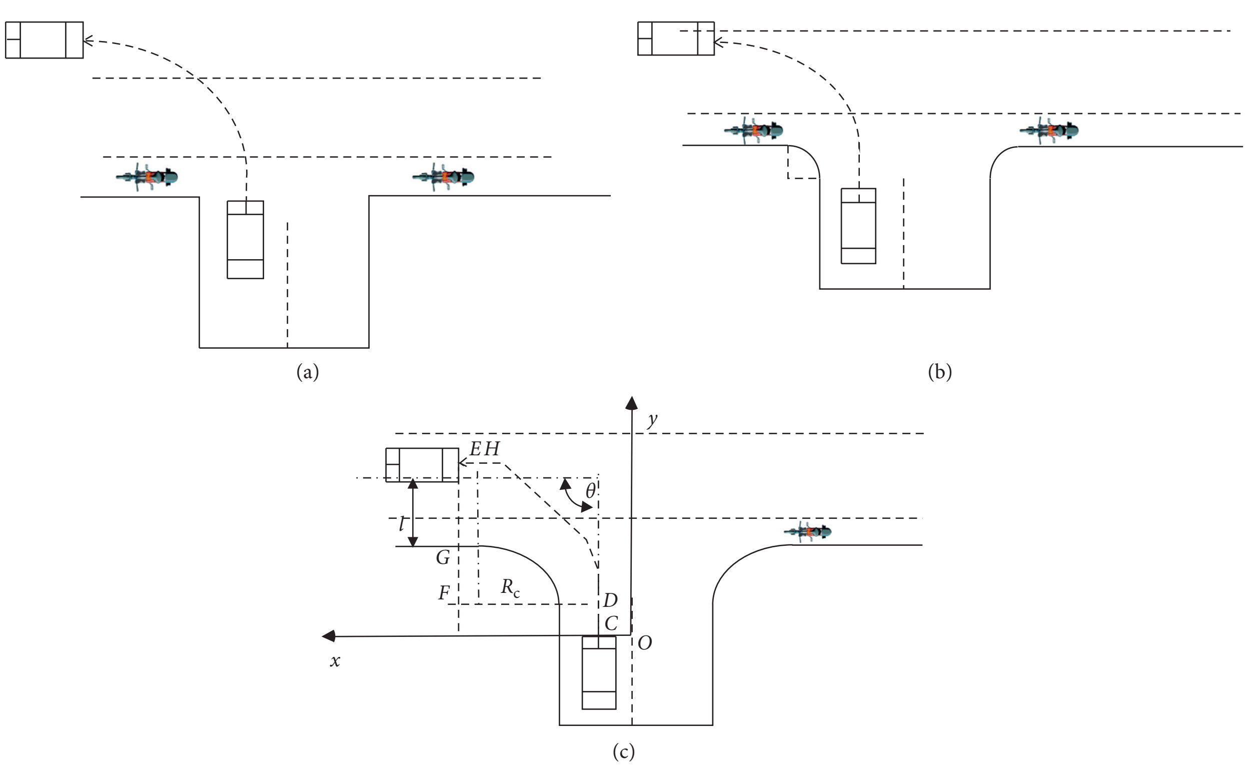

Figure 14: Left turns on the driveway. (a) Driveway without exiting radius. (b) Driveway with small exiting radius. (c) Driveway with large exiting radius.

From Figures 13 and 14, we assume that V_C is the same as V_{dd}, V_E is the same as V_{du}, and x_D is one quarter of W, and then we obtain the following formulas:

$$l = \frac{W_{lu}}{2} + W_{nv}, \quad (37)$$

$$EG - l + \frac{W_{veh}}{2} = \frac{W_{lu}}{2}, \quad (38)$$

$$EG = \left(b' \ln x_E + \frac{c'V_E^2}{3.6^2} + \frac{d'V_E}{3.6}\right) - \left(b' \ln x_D + \frac{c'V_D^2}{3.6^2} + \frac{d'V_D}{3.6}\right) - R_c, \quad (39)$$

$$x_E = R_c + \frac{W}{2} + \frac{V_E^2 - V_H^2}{2 \times 3.6^2 a_{EH}}. \quad (40)$$

Combining equations (25) and (32) to (40), we obtain the following formulas for R_c:

$$W_{lu} - \frac{W_{veh}}{2} + W_{nv} \le \left[b' \ln\left(R_c + \frac{W}{2} + \frac{V_{du}^2 - V_H^2}{2 \times 3.6^2 a_{EH}}\right) + \frac{c'V_{du}^2}{3.6^2} + \frac{d'V_{du}}{3.6}\right] - \left[b' \ln\left(\frac{W}{4}\right) + \frac{c'\left(V_{dd} - 10\right)^2}{3.6^2} + \frac{d'\left(V_{dd} - 10\right)}{3.6}\right] - R_c, \quad (41)$$

$$b' = -0.3997 R_c N - 11.431\left(\frac{W_{lu}}{2} + W_{nv}\right) + 0.1354 R_c^2 + 32.5615, \quad (42)$$

$$c' = 0.0923 + 0.086 R_c - 0.412\left(\frac{W_{lu}}{2} + W_{nv}\right) N + 0.012 R_c^2, \quad (43)$$

$$d' = 2.214 R_c - 1.123 R_c^2 - 53.976. \quad (44)$$

5. Design Evaluation and Optimization

With equations (4), (9), (13), (17), (28) to (31), and (41) to (44), we can calculate alternative ranges of driveway width and curb radius, and then, by considering the requirement of the guide [29], we can adjust the alternative ranges to get better ranges for field conditions.

Models of driveway width and curb radius are from the perspective of crash risk. The purpose of driveway width models is reducing the crash risk caused by conflicts between left-turning and through vehicles, conflicts between right-turning and through vehicles, and conflicts between motorized and nonmotorized traffic. Meanwhile, the purpose of curb radius models is reducing the crash risk caused by lane encroachment and speed differential. Consequently, to verify the traffic safety effects of the design models, we establish a model for optimizing the combination of driveway width and curb radius in alternative ranges, with respect to traffic safety indexes, such as traffic conflicts, lane encroachment, and speed differential, as follows:

$$P_{WR} = P_{vv} + P_{mn} + P_{sd} + P_{le}, \quad (45)$$

where P_{WR} is the crash risk with one combination of driveway width and curb radius (%); P_{vv} is the crash risk from conflicts between motorized vehicles (%); P_{mn} is the crash risk from conflicts between motorized and nonmotorized traffic (%); P_{sd} is the crash risk due to speed differential larger than 10 km/h (%); P_{le} is the crash risk from lane encroachment of entering and exiting vehicles (%).

5.1. Definitions. P_{vv} is estimated as follows [26]:

$$P_{vv} = \frac{N_{tc}}{N_{pcu}}, \quad (46)$$

where N_{tc} is the number of motorized traffic conflicts in the peak hour; N_{pcu} is the Passenger Car Equivalent values of motorized traffic in the peak hour.

Similarly, we define P_{mn}, P_{sd}, and P_{le} as follows:

$$P_{mn} = \frac{N_{tcn}}{\left(N_{pcu} + N_{nt}\right)}, \quad (47)$$

where N_{tcn} is the number of traffic conflicts between motorized and non-motorized traffic; N_{nt} is the number of nonmotorized traffic in the peak hour; and

$$P_{sd} = \frac{N_{sd}}{N_{pcu}}, \quad (48)$$

where N_{sd} is the number of speed differentials larger than 10 km/h in the peak hour; and

$$P_{le} = \frac{N_{le}}{N_{pcu}}, \quad (49)$$

where N_{le} is the number of lane encroachments in the peak hour.

N_{tc}, N_{pcu}, N_{tcn}, N_{nt}, N_{sd}, and N_{le} are calculated in functional areas of the driveway, comprised of four parts, upstream and downstream functional areas of SCS and upstream and downstream functional areas of driveway, as shown in Figure 15.

Then we can utilize the VISSIM microscopic traffic analysis software to develop statistics for functional areas of driveways. In VISSIM [31], we use function "Vehicle Inputs" to obtain N_{pcu} and N_{nt}, function "Speed Difference" to get N_{sd}, and function "Lane Change" to obtain N_{le}.

A traffic conflict is a traffic event involving the interaction of two or more road users, where one or both drivers take evasive action such as braking or swerving to avoid a collision [32]. Therefore, we can identify traffic conflicts by analyzing the interaction status of two or more road users. In VISSIM, function "Vehicle Record" outputs attribute values for each vehicle as raw data in one row per time step, which provides the moving status of individual vehicle. Then we

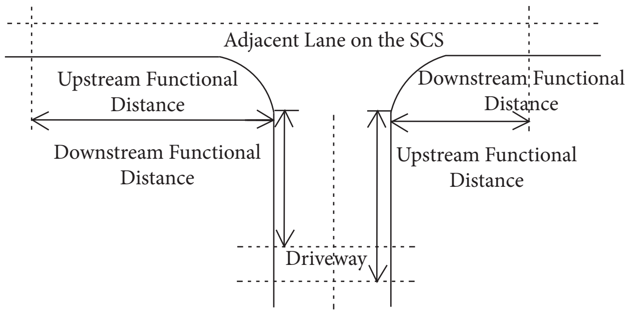

Figure 15: Functional area of the driveway.

can recognize the traffic conflicts by counting data from function "Vehicle Record." First of all, we use subfunction "interaction state" in "Vehicle Record," which can demonstrate the interaction of vehicles. If the value of "interaction state" is Brake BX, Brake AX, Close up, Brake ZX, Brake SPW, Brake COOP, or Pass [31], the vehicle is influenced by others, so we can judge that the raw data of the row from "Vehicle Record" file shows the traffic conflict has happened. Secondly, based on vehicle interactions, we use subfunctions "Acceleration," "Number of Stops," and "Lane Change" which provide values of evasive actions, such as acceleration, stop number, and lane change, to reconfirm that those row data are phenomenon of traffic conflicts. Thirdly, we count the number of those rows, that is, the number of traffic conflicts in the peak hour. Finally, with subfunctions "Lane" (number of lanes on which the vehicle is used) and "Position" (distance on the link from the beginning of the link or connector), which present locations where traffic conflicts happen, we can divide the number of traffic conflicts into the number of motorized traffic conflicts N_{tc} and the number of traffic conflicts between motorized and nonmotorized traffic N_{tcn}.

For example, we may obtain sample attribute values from the $*$.fzp file of "Vehicle Record," as shown in Table 1.

According to the discussion above, from Table 1, we can see that the 1_{st}, 2_{nd}, 3_{rd}, 5_{th}, 7_{th}, 8_{th}, 9_{th}, and 10_{th} rows are phenomenon of traffic conflicts, so the number of traffic conflicts is 8. Then as the crosswalk for nonmotorized traffic is 63.320 m from the beginning of the link, 7_{th} and 10_{th} rows present traffic conflicts happening at the edge of crosswalk, which are conflicts between motorized and nonmotorized traffic. Consequently, N_{tc} is 6 and N_{tcn} is 2 in this example.

5.2. Regression Models and Programming. In VISSIM, we design different combinations of driveway width and curb radius for various traffic volumes on the SCS and the driveway, to investigate the relationship among the crash risk, driveway width, and curb radius. We use a range of values of driveway width and curb radius based on driveway guide [29], as shown in Table 2.

Note: we assume that the driveway has only two lanes.

From Table 2, we can see that there are 121 pairs of driveway width and curb radius. Based on simulation results, each pair of driveway width and curb radius corresponds to different values of P_{vv}, P_{mn}, P_{sd}, and P_{le}. Consequently, we can derive regression models to describe the relationship of crash risk and design factors. The regression models show that $P_{\mathrm{vv}} = f_1(W, R_{\mathrm{c}})$, $P_{\mathrm{mn}} = f_2(W, R_{\mathrm{c}})$, $P_{\mathrm{sd}} = f_3(R_{\mathrm{c}}, W)$, and $P_{\mathrm{le}} = f_4(R_{\mathrm{c}}, W)$, meaning that these four types of crash risk are functions of driveway width and curb radius.

Consequently, we first obtain the alternative ranges of W and R_{c} by using Matlab to program equations (4), (9), (13), (17), (28) to (31), and (41) to (44) and then use equation (45) for P_{WR}, which combines these regression models, to verify the alternative ranges of W and R_{c}, and find the optimal pair.

6. Case Study Evaluation

Field survey and sample data were collected from 6:00 pm to 7:00 pm on June 29, 2019, at Wanda Plaza, Cangshan District, Fuzhou City, China. Wanda Plaza is a type of superblock called city complex with dimensions of approximately 290m × 580m. There are business centers, pedestrian streets, high end hotels, office buildings, and residential apartments as well as retail, catering, cultural, and entertainment venues.

(1) There are many pedestrians and nonmotorized vehicles crossing the driveways, which contribute to traffic congestion and elevated traffic safety risk

(2) A basic design of driveways yields adverse impacts in the efficiency of turning movements of vehicles

The driveway and adjacent road system of Wanda Plaza are shown in Figure 16. Features of these driveways are shown in Table 3 and Figure 17. Driveways 9 and 10 are toward different destinations, so we separate them into two driveways, as illustrated in Figure 17(i).

The driveway width and curb radius models need some basic traffic data. According to these design models, we list the data source in Tables 4–6. For traffic volume data, we collect and count the number of different kinds of traffic and then obtain the traffic volume, as shown in Table 4. For other driveway traffic data, we found the design drawings and took video pictures of traffic flow in real field. Then we acquired the driveway slope, longitudinal friction coefficient, and lane width from design drawings and obtained radii of turning trajectories, number of traffic conflicts, included angle of trajectories, and required velocities by analyzing the video pictures taken from the real field, as shown in Table 5. For assumed data, we list the assumed values and their data source in Table 6.

Note: "$*$" denotes assumed value; "—" denotes that parameter is not needed.

Based on the applicable conditions at Wanda Plaza superblock, we combine equations to optimize the driveways as shown in Table 7.

Note: "—" indicates currently no model available for movements on this type of driveway. For driveways 3 and 4, there is no movement 1 or 2 in Figures 9 and 10, so no curb radius model can be used for them. For driveways 8 to 10, there are no exiting movements in Figure 3, so no driveway width model is fit for them.

Table 1: Sample attribute values for each vehicle from "Vehicle Record."

Simulation second (s)	Number of the vehicles	Interaction state	Acceleration (m/s^2)	Number of stops	Lane change	Lane	Position (m)
1982.60	1240	Brake BX	−0.02	0	None	1–1	48.269
1982.60	1241	Close up	−2.17	0	None	1–1	19.259
1982.60	1242	Brake AX	−0.02	0	None	1–1	57.598
1982.60	1243	Free	0.19	0	None	1–1	94.569
1982.70	1230	Pass	−2.31	1	Left	1–1	32.926
1982.70	1236	Free	0.13	0	None	2–1	34.658
1982.80	1232	Close up	−1.37	0	None	2–1	62.320
1982.70	1237	Close up	−1.93	1	None	2–1	15.425
1982.70	1238	Brake ZX	−6.65	0	Right	1–1	46.720
1982.80	1239	Close up	−0.45	0	None	2–1	62.320

Table 2: Alternative values of driveway width and curb radius.

Driveway lane width W_{lane} (m)	3	3.25	3.5	3.75	4	4.25	4.5	4.75	5	5.25	5.5
Driveway width W (m)	6	6.5	7	7.5	8	8.5	9	9.5	10	10.5	11
Curb radius R_c (m)	10	15	20	25	30	35	40	45	50	55	60

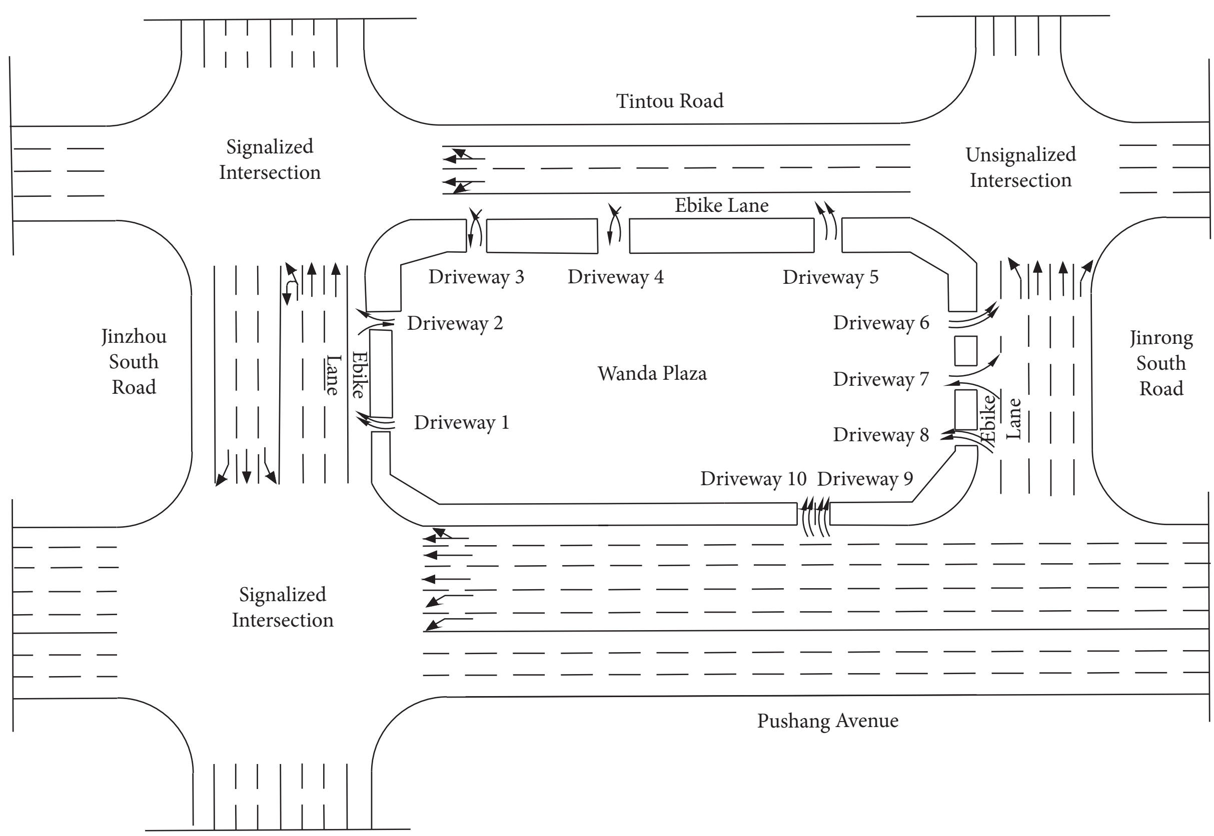

Figure 16: Driveway system of Wanda Plaza.

Let us take driveway 1 as an example. As Table 7 indicates, we program equations (9), (13), (17), and (41) to (44) in Matlab and input data from Tables 5 and 6. Then combining the output of Matlab program above and alternative design values from Table 2, the following design range for driveway 1 is produced. Following the same process, we calculate separate design ranges for the driveways, as shown in Table 8.

We use VISSIM to simulate the different combinations of driveway width and curb radius for various traffic volumes on the SCS and the driveway, so as to obtain conflict results, that is, values of crash risk, for polynomial regression

Table 3: Current design of driveways.

Driveway number	Number of lanes	Lane direction	Control measure	Width W (m)	Curb radius R_c (m)
1	2	Entrance lanes	No control	8	0
2	2	One entrance lane and one exit lane	No control	8	18
3	2	One entrance lane and one exit lane	Barrier control	6	25
4	2	One entrance lane and one exit lane	Barrier control	7	0
5	2	Exit lanes	No control	4.5	20
6	2	Exit lanes	Barrier control	6	15
7	2	One entrance lane and one exit lane	Barrier control	6	0
8	2	Entrance lanes	Barrier control	7.5	15
9	2	Entrance lanes	No control	7	20
10	2	Entrance lanes	No control	7	20

Figure 17: Wanda Plaza driveways. (a) Driveway 1. (b) Driveway 2. (c) Driveway 3. (d) Driveway 4. (e) Driveway 5. (f) Driveway 6. (g) Driveway 7. (h) Driveway 8. (i) Driveways 9 and 10.

Table 4: Traffic volume from 6:00 pm to 7:00 pm on June 29, 2019

Driveway number	1	2	3	4	5	6	7	8	9	10
Crossing pedestrians (ped/h)	292	268	328	416	120	96	180	216	531	415
Crossing nonmotorized vehicles (veh/h)	364	224	236	168	88	132	244	324	279	281
Motorized vehicles on the adjacent urban lane (pcu/h)	580	628	288	200	294	64	332	474	692	692
Motorized vehicles on the driveway (pcu/h)	380	400	88	52	168	84	44	156	254	362

Table 5: Other collected driveway traffic data.

Driveway number	1	2	3	4	5	6	7	8	9	10
i'	0	0	0	0	0	0	0	—	—	—
N (h^{-1})	15	18	—	—	8	9	11	16	25	21
R_l (m)	—	—	17	18	14	18	16	—	—	—
R_r (m)	8	12	—	—	—	—	—	—	—	—
V_{ae} (km/h)	6.72	7.68	8.05	7.52	7.32	8.21	6.43	—	—	—
V_{dd} (km/h)	20	25	25	25	25	25	20	20	20	20
V_{du} (km/h)	50	50	30	30	30	40	40	40	60	60
V_H (km/h) (SCS)	35	36	—	—	21	28	29	—	—	—
V_H (km/h) (driveway)	—	17	—	—	—	—	15	15	18	13
V_{nm} (km/h)	12	15	15	13	22	20	13	—	—	—
V_p (km/h)	4.91	4.12	5.01	4.82	3.41	5.35	4.70	—	—	—
W_{cro} (m)	3	3	4	4	4	3	5	—	—	—
W_{lu} (m)	3.5	3.5	—	—	3.5	3.5	3.5	3.5	3.5	3.5
W_{nv} (m)	2.5	2.5	3	3	3	3	3	3	3	3
W_{veh} (m)	1.8	1.8	1.8	1.8	1.8	1.8	1.8	1.8	1.8	1.8
δ (rad)	0.6981	1.0472	—	—	—	—	—	—	—	—
φ	0.6	0.6	0.6	0.6	0.6	0.6	0.6	—	—	—

Table 6: Assumed values for driveway traffic analysis.

Driveway number	Source	1	2	3	4	5	6	7	8	9	10
a_{EH} (m/s^2)	[33]	1.5	1.5	—	—	1.5	1.5	1.5	1.5	1.5	1.5
l_0 (m)	[26]	3	3	3	3	3	3	3	—	—	—
t_{cl} (s)	[34]	—	—	5.77	5.77	5.77	5.77	5.77	—	—	—
t_{cr} (s)	[34]	2.94	2.94	—	—	—	—	—	—	—	—
t_{mn} (s)	*	3.5	3.5	3.5	3.5	3.5	3.5	3.5	—	—	—
t_{pr} (s)	[26]	1.2	1.2	1.2	1.2	1.2	1.2	1.2	1.2	1.2	1.2
t_{vp} (s)	[35]	4.4	4.4	4.4	4.4	4.4	4.4	4.4	—	—	—

Table 7: Relationship between driveways and design models.

Driveway number	Width optimization models	Curb radius optimization models
1	Equations (9), (13), and (17)	Equations (41) to (44)
2	Equations (9), (13), and (17)	Equations (28) to (31) and (41) to (44)
3	Equations (4), (13), and (17)	—
4	Equations (4), (13), and (17)	—
5	Equations (4), (13), and (17)	Equations (41) to (44)
6	Equations (4), (13), and (17)	Equations (41) to (44)
7	Equations (4), (13), and (17)	Equations (28) to (31) and (41) to (44)
8	—	Equations (28) to (31)
9	—	Equations (28) to (31)
10	—	Equations (28) to (31)

Table 8: Alternative driveway design range.

Driveway number	Range of driveway width W (m)	Range of curb radius R_c (m)
1	$6 \le W \le 8$	$10 \le R_c \le 50$
2	$6 \le W \le 8.5$	$15 \le R_c \le 55$
3	$6 \le W \le 9$	25
4	$6 \le W \le 10$	0
5	$6 \le W \le 8$	$15 \le R_c \le 60$
6	$6 \le W \le 9$	$10 \le R_c \le 45$
7	$6 \le W \le 8.5$	$10 \le R_c \le 50$
8	7.5	$20 \le R_c \le 55$
9	7	$15 \le R_c \le 60$
10	7	$20 \le R_c \le 60$

models. Some relevant parameters are set in accordance with the driving characteristics of local drivers in VISSIM simulator, for example, various speed, and others are set from references, for example, acceleration rate, minimum gap, and perception-reaction time.

To verify the validity of simulation, we add one comparison of the simulation results with the actual observed results. Firstly, we choose driveway 1 of Fuzhou Wanda Plaza as an example and then count traffic conflicts by personal judgment on video pictures of real field. Secondly, we simulate the current situation of driveway 1 and then recognize traffic conflicts in VISSIM simulation. Finally, we compare the traffic conflict results from simulation and actual observation of driveway 1, as shown in Table 9.

From Table 9, we find that the difference rate of simulation and actual observation of driveway 1, is less than 5%. By using the same method, we compare the results of simulation and actual observation of driveway 2 to 10 and get the same result that difference rates are less than 5%. So we can draw a conclusion that simulation results are acceptable. Therefore, by using traffic volumes from Table 4 and driveway width and curb radii from Table 2, we perform simulation in VISSIM. Taking driveway 1 as an example, we obtain values for variables in the crash risk models. Then, by using formulas (46) to (49), we calculate P_{vv}, P_{mn}, P_{sd}, and P_{le} and deduce polynomial regression models for driveway 1 as follows:

$$P_{\mathrm{vv}} = 1.66 - 6.10e^{-1}W - 3.90\mathrm{e}^{-3}R_{\mathrm{c}} + 7.63\mathrm{e}^{-2}W^2 + 3.64\mathrm{e}^{-4}WR_{\mathrm{c}} + 4.86\mathrm{e}^{-5}R_{\mathrm{c}}^2 - 3.03\mathrm{e}^{-3}W^3 - 2.21\mathrm{e}^{-5}W^2R_{\mathrm{c}} - 3.456\mathrm{e}^{-7}WR_{\mathrm{c}}^2 - 2.59\mathrm{e}^{-8}R_{\mathrm{c}}^3, \quad (50)$$

$$P_{\mathrm{mn}} = 2.87\mathrm{e}^{-1} - 1.13\mathrm{e}^{-1}W - 8.80e^{-4}R_{\mathrm{c}} + 1.46\mathrm{e}^{-2}W^2 + 3.01\mathrm{e}^{-4}WR_{\mathrm{c}} - 7.20\mathrm{e}^{-7}R_{\mathrm{c}}^2 - 5.80\mathrm{e}^{-4}W^3 - 2.55\mathrm{e}^{-5}W^2R_{\mathrm{c}} + 2.23\mathrm{e}^{-6}WR_{\mathrm{c}}^2 + 3.73\mathrm{e}^{-8}R_{\mathrm{c}}^3, \quad (51)$$

$$P_{\mathrm{sd}} = 8.76\mathrm{e}^{-1} - 2.92\mathrm{e}^{-1}W - 3.00\mathrm{e}^{-3}R_{\mathrm{c}} + 3.54\mathrm{e}^{-2}W^2 + 2.86\mathrm{e}^{-4}WR_{\mathrm{c}} + 3.33\mathrm{e}^{-6}R_{\mathrm{c}}^2 - 1.38\mathrm{e}^{-3}W^3 - 1.21\mathrm{e}^{-5}W^2R_{\mathrm{c}} - 6.91\mathrm{e}^{-7}WR_{\mathrm{c}}^2 + 4.74\mathrm{e}^{-7}R_{\mathrm{c}}^3, \quad (52)$$

$$P_{\mathrm{le}} = 9.38\mathrm{e}^{-1} - 3.46\mathrm{e}^{-1}W + 1.62\mathrm{e}^{-3}R_{\mathrm{c}} + 4.35\mathrm{e}^{-2}W^2 - 8.68\mathrm{e}^{-4}WR_{\mathrm{c}} + 5.40\mathrm{e}^{-5}R_{\mathrm{c}}^2 - 1.75\mathrm{e}^{-3}W^3 + 5.06\mathrm{e}^{-5}W^2R_{\mathrm{c}} - 8.19\mathrm{e}^{-7}WR_{\mathrm{c}}^2 - 1.16\mathrm{e}^{-7}R_{\mathrm{c}}^3. \quad (53)$$

And we also analyze the goodness of fit of these curve fitting equations, indicating that they are suitable for scatter fitting, as shown in Table 10.

For driveway 1, we combine equations (50) to (53) to obtain the optimization function, based on equation (45), as follows:

$$P_{\mathrm{WR}} = 3.76 - 1.36W - 6.16\mathrm{e}^{-3}R_{\mathrm{c}} + 1.70\mathrm{e}^{-1}W^2 + 8.31\mathrm{e}^{-5}WR_{\mathrm{c}} + 1.05\mathrm{e}^{-4}R_{\mathrm{c}}^2 - 6.74\mathrm{e}^{-3}W^3 - 9.11\mathrm{e}^{-6}W^2R_{\mathrm{c}} + 3.71\mathrm{e}^{-7}WR_{\mathrm{c}}^2 + 3.69\mathrm{e}^{-7}R_{\mathrm{c}}^3. \quad (54)$$

The diagram of the relationship among P_{WR}, W, and R_{c} is shown in Figure 18.

By using a similar process, we estimate polynomial regression models for driveways 2 to 10, which are shown in Figure 19.

The outcomes shown in Figures 18 and 19 suggest the following key findings for driveway radius and width:

(1) Optimization for W and R_{c}: for driveways 1, 2, 5, 6, and 7, the value of P_{WR} decreases at first and then increases, with an increase of R_{c}. However, for driveways 1 and 2, the value of P_{WR} increases at first and then decreases, with an increase of W, while for driveways 5, 6, and 7, the value of P_{WR} decreases at first and then increases, with an increase of W. Consequently, we can see that a certain range of curb radius and driveway width would lead to lower crash risk. The reason for it is that, for driveways 1 and 2, traffic volume of either nonmotorized vehicles or motorized vehicles is relatively high, so that P_{vv} and P_{mn} have a large impact on P_{WR}, which means that a smaller driveway width and larger curb radius would be better, but for driveways 5, 6, and 7, the traffic volume is relatively low, so P_{vv} and P_{mn} have a small impact on P_{WR}, which means that a larger driveway width and curb radius work better. However, when the curb radius or driveway width is too large, there will be a longer pedestrian crossing area, leading to more crash risk.

(2) Optimization for W: for driveways 3 and 4, while R_{c} is the fixed value, the value of P_{WR} decreases at first and then increases, with an increase of W, meaning that a certain range of driveway width would lead to lower crash risk. The reason for it is that the traffic volume of either nonmotorized or motorized vehicles in functional areas of these driveways, as shown in Table 4, is relatively low, so that P_{vv} and P_{mn} have a small impact on P_{WR}, but P_{sd} and P_{le} have large influence on P_{WR}, which means that a larger

Table 9: Comparison of simulation and actual observation of driveway 1.

Conflict results	Number of motorized traffic conflicts in the peak hour N_{tc}	Number of traffic conflicts between motorized and nonmotorized traffic N_{tcn}	Number of speed differentials larger than 10 km/h in the peak hour N_{sd}	Number of lane encroachments in the peak hour N_{le}
Actual observation	182	44	113	55
Simulation	189	42	108	57
Difference rate	3.85%	−4.55%	−4.42%	3.64%

Table 10: Goodness of fit of equations.

Indices of goodness of fit	Sum of squared errors (SSE)	R^2	Root mean squared error (RMSE)
Equation (50)	0.002368	0.9544	0.004619
Equation (51)	0.0005933	0.9761	0.002312
Equation (52)	0.003296	0.9179	0.005449
Equation (53)	0.003485	0.9106	0.005013

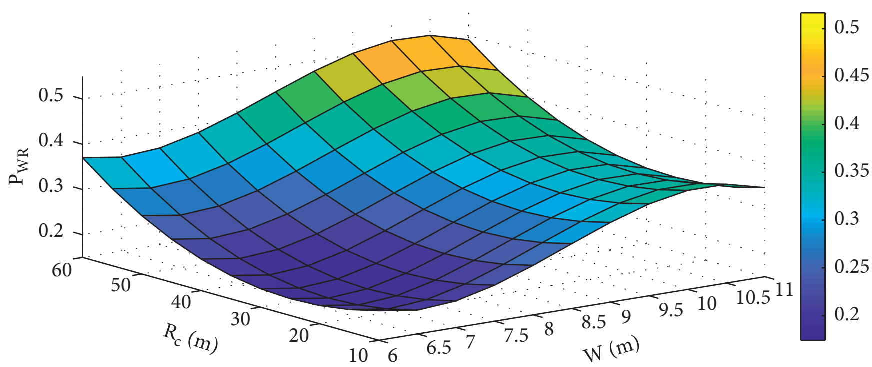

Figure 18: Curve of relationship among P_{WR}, W, and R_c for driveway 1.

driveway width would be better. However, same as above, when the driveway width is too large, there is more crash risk among vehicles and pedestrians.

(3) Optimization for R_c: for driveways 8, 9, and 10, while W is the fixed value, the value of P_{WR} decreases at first and then increases, with an increase of R_c, meaning that a certain range of curb radius would lead to lower crash risk. The reason for it is that the traffic volume of either nonmotorized or motorized vehicles is relatively high, so that the values of P_{sd} and P_{le} are large, which means that a larger curb radius would be better. However, same as above, when the curb radius is too large, there is more crash risk among vehicles and pedestrians.

(4) Traffic volumes are closely related to the value of P_{WR}. Higher traffic volumes normally yield more crash risk.

Based on Table 8, we find the optimal driveway design for driveways, as shown in Table 11, by using the regression models for P_{WR}.

Compared with the current design, the updated design will reduce crash risk by 4.32% to 52.61%, with 7 out of 10 driveways improving by 16.14% or more, as shown in Table 12. As the effectiveness of access management strategies is location-specific, indicated by Chowdhury et al. [22], there are large differences among improvements of driveways.

7. Discussion and Limitations

In this research, we put forward driveway width models, based on conflicts between left-turning and through vehicles, conflicts between right-turning and through vehicles, and conflicts between motorized and nonmotorized traffic. The width values calculated by the models would help turning vehicles and nonmotorized traffic make full use of the gap, so as to reduce the crash risk from conflicts between motorized vehicles P_{vv}, and the crash risk from conflicts between motorized and nonmotorized traffic P_{mn}. The models can be used for acquiring the range of driveway width of superblocks. At the same time, we propose curb radius models, aiming to reduce the speed differential and avoid lane encroachment. The curb radius values calculated by the models are beneficial for reducing the crash risk due to speed differential larger than 10 km/h P_{sd} and the crash risk from lane encroachment of entering and exiting vehicles

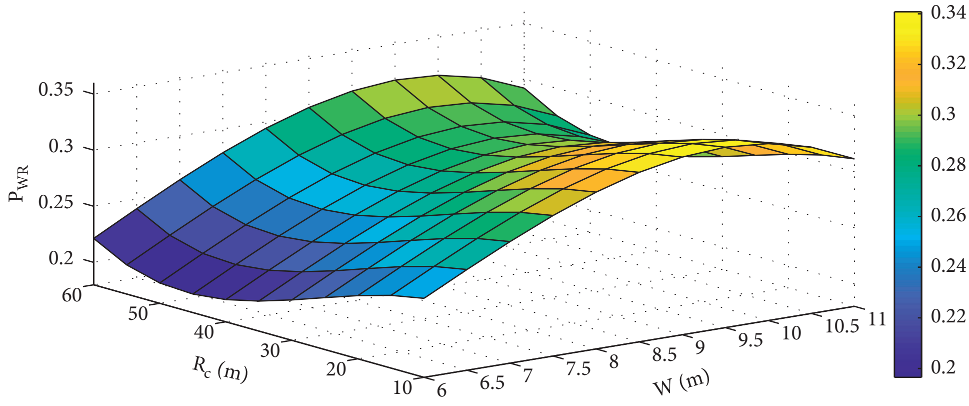

(a)

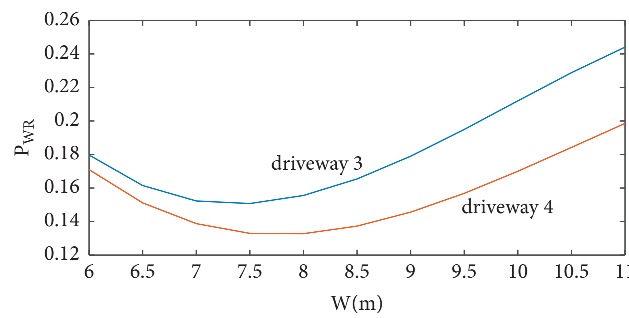

(b)

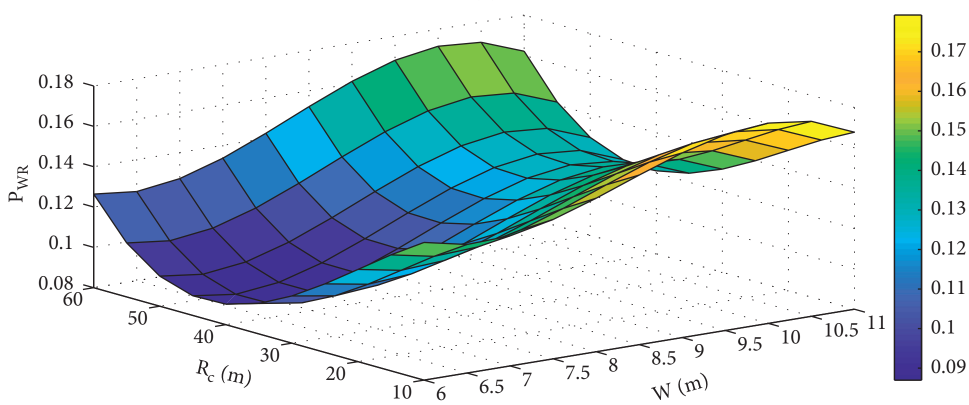

(c)

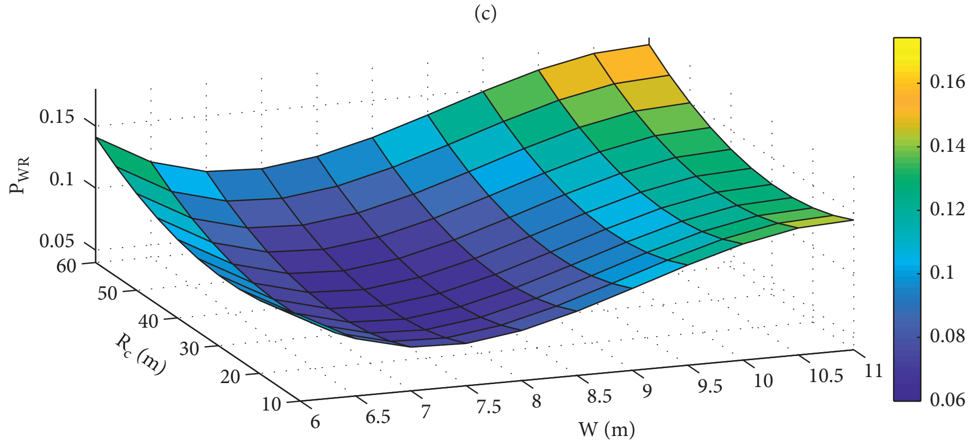

(d)

FIGURE 19: Continued.

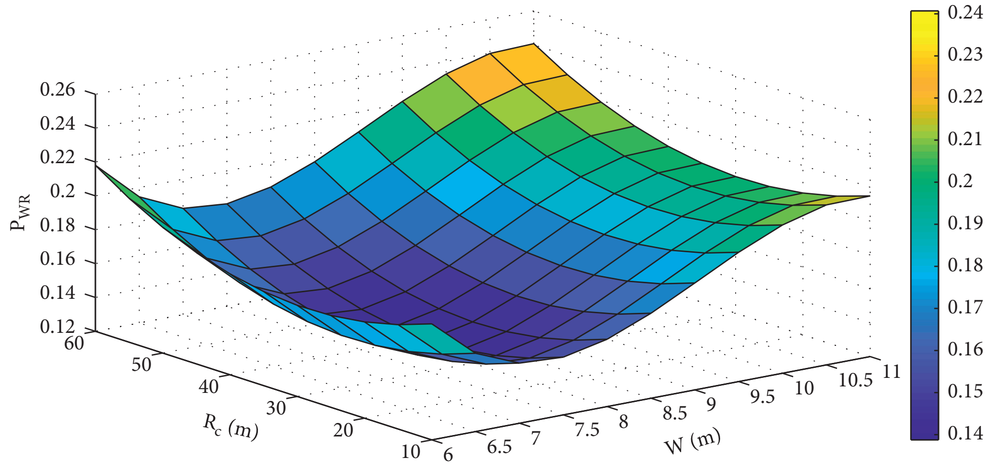

(e)

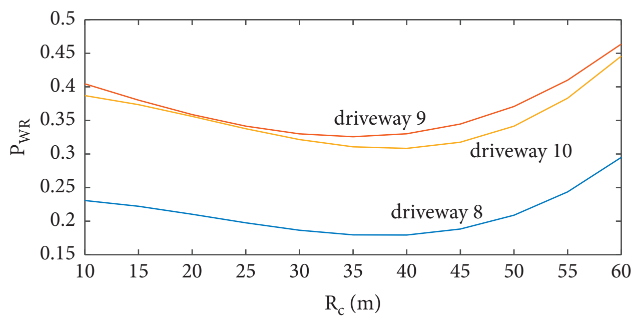

(f)

FIGURE 19: Curves of relationship among P_{WR}, W, and R_c for driveways. (a) Driveway 2. (b) Driveways 3 and 4. (c) Driveway 5. (d) Driveway 6. (e) Driveway 7. (f) Driveways 8, 9, and 10.

TABLE 11: Optimal driveway design.

Driveway number	Driveway width W (m)	Curb radius R_c (m)
1	6.5	30
2	6	45
3	7.5	25
4	8	0
5	6.5	45
6	7.5	30
7	7	30
8	7.5	35
9	7	35
10	7	40

TABLE 12: Crash risk P_{WR} comparison.

Driveway number	Current driveway design	Optimal driveway design	Improvement (%)
1	0.3091	0.1780	42.41%
2	0.3098	0.1965	36.57%
3	0.1797	0.1507	16.14%
4	0.1388	0.1328	4.32%
5	0.1836	0.0870	52.61%
6	0.1031	0.0599	41.90%
7	0.2087	0.1403	32.77%
8	0.2222	0.1796	19.17%
9	0.3802	0.3257	14.33%
10	0.3560	0.3083	13.40%

P_{le}. The models can be used for acquiring the range of curb radius of superblocks.

The models of driveway width and curb radius optimize the driveway width and curb radius from the perspective of crash risk based on traffic safety indexes. However, the models should not neglect the capacity demand of SCS and driveway, which is the basis for improving traffic efficiency. Therefore, future research will focus on the driveway width and curb radius models based on traditional models corresponding to traffic volume and speed, for example, traffic arrival models based on the traffic wave theory [36], to heighten the level of both safety and efficiency. Meanwhile, the models assume that the starting position and traffic trajectories are fixed, but the starting position may be flexible, and shapes of traffic trajectories in real situation are variable and more complicated. Further research is needed to investigate the impact of different positions and trajectories on the driveway width and curb radius. Additionally, driveway width models for avoiding conflicts between motorized and nonmotorized traffic give consideration to both traffic safety and land resources, but the consideration is qualitative and hypothetical. In the future, we will pay more attention to the quantitative analysis of relationship of land use efficiency and traffic safety.

We also provide the crash risk models, which can be used for evaluating the alternative ranges of driveway width and curb radius, and find the optimal pair. The models will give the safety effect of different design schemes and provide the safest design. However, these evaluation models have not considered the capacity effects yet, which should be studied in the future research.

We measured and obtained the data from one superblock from 6:00 pm to 7:00 pm on June 29, 2019. As the data size is small, we used the data directly for design models and did not preprocess data and check the accuracy of the data in advance. In the future research, we should obtain adequate data size in more superblocks and then preprocess the data and check the accuracy of the data, so as to ensure the validity of the design models.

8. Conclusions

Current guidelines for driveway design and traffic safety provide reference values and qualitative guidance. Superblock driveways generate a busy and complex traffic environment, which requires detailed quantitative models for design, evaluation, and permitting. Driveway width and curb radius are key factors of driveway design. Recent research indicates that these two design factors are closely connected. This paper investigates and develops models of driveway width and curb radius and proposes crash risk models for design evaluation and optimization.

Driveway width models are based on conflicts between exiting turns and through flow, the interaction between motorized and nonmotorized traffic, and the competition for available and acceptable gaps. The developed models can calculate a range of driveway widths, given their turning movements. The updated driveway width estimates can reduce traffic conflicts between exiting turn and through vehicles and decrease the number of conflicts between exiting vehicles and crossing nonmotorized traffic.

Curb radius models account for turning paths, speed differential, and lane encroachment. The updated models connect the driveway width and curb radius, and they can produce a range of curb radius estimates for driveways with entering and exiting movements. Also, the updated curb radius can decrease the number of speed differences larger than 10 km/h and lane encroachments.

The crash risk models account for traffic conflicts, speed differential, and lane encroachment. The relationships among crash risk, driveway width, and curb radius are represented with polynomial regression models. The results indicate that (i) larger curb radius and smaller driveway width would lead to lower crash risk, when traffic volumes are high; (ii) larger curb radius and driveway width would lead to lower crash risk, when traffic volumes are low; (iii) when curb radius or driveway width is too large, a higher crash risk is possible; and (iv) higher traffic volumes increase crash risk.

Finally, we find that design ranges by using the proposed models are reasonable and effective; compared with the current design, the updated design reduces crash risk. Although the steps of analysis and formulas for driveway design and evaluation are complex, the method can be automated by computer programming and the required inputs for solving the problem are modest, as shown by the data in Tables 4, 5, and 6.

Data Availability

All data used to support the findings of this study are included within the article.

Conflicts of Interest

The authors do not have conflicts of interest with other entities or researchers.

Acknowledgments

The authors would like to thank Lulu Tang, Tianhe Li, and Jinmeng Chen from Fuzhou University, China, and Jing Chen from Tongji University, China, for their support and assistance.

References

[1] M. E. Agnes, *Webster's New World College Dictionary*, John Wiley & Sons, Hoboken, NJ, USA, 1999.

[2] H. Y. Kan, A. Forsyth, and P. Rowe, "Redesigning China's superblock neighbourhoods: policies, opportunities and challenges," *Journal of Urban Design*, vol. 22, no. 6, pp. 757–777, 2017.

[3] R. Ewing, D. Choi, F. Kiani, J. Kim, and S. Sabouri, *Street Network Connectivity, Traffic Congestion, and Traffic Safety*, Utah Department of Transportation Research & Innovation Division, Salt Lake City, Utah, USA, 2020.

[4] K. M. Williams, V. G. Stover, K. K. Dixon, and P. Demosthenes, *Access Management Manual*, Transportation Research Board, Washington, D.C., USA, 2014.

[5] W. E. Frawley and W. L. Eisele, “Access Management Guidebook for Texas,” Transportation Institute of Texas A&M University System, Austin, TX, USA, FHWA/TX-05/0-4141-P3, 2005.

[6] Planning & Zoning Center, Inc, *Reducing Traffic Congestion and Improving Traffic Safety in Michigan Communities: The Access Management Guidebook*, Michigan Department of Transportation, Lansing, MI, USA, 2001.

[7] V. Department of Transportation, *Access Management Regulations*, Richmond, virginia, USA, 2013.

[8] J. Gluck, H. S. Levinson, and V. Stover, “Impacts of Access Management Techniques,” NCHRP Report 420, Transportation Research Board, Washington, D.C., USA, 1999.

[9] American Association of State Highway and Transportation Officials (Aashto), *A Policy on Geometric Design of Highways and Streets*, AASHTO, Washington, D.C., USA, 2018.

[10] National Cooperative Highway Research Program (NCHRP), “Public Liabilities Relating to Driveway Permits. NCHRP 20-06/Topic 25-01,” 2019, https://apps.trb.org/cmsfeed/TRBNeProjectDisplay.asp? ProjectID=4811.

[11] M. Chakraborty and T. J. Gates, “Association between driveway land use and safety performance on rural highways,” *Transportation Research Record: Journal of the Transportation Research Board*, vol. 2675, no. 1, pp. 114–124, 2021.

[12] J. L. Gattis, J. S. Gluck, J. M. Barlow, R. W. Eck, W. F. Hecker, and H. S. Levinson, “Guide for the Geometric Design of Driveways,” Transportation Research Board, Washington, D.C., USA, NCHRP Project 659, 2010.

[13] G. Sokolow, V. Stover, F. Broen, and A. Datz, *Driveway Information Guide*, Florida Department of Transportation, Tallahassee, FL, USA, 2008.

[14] Y. Zou, B. Lin, X. Yang, L. Wu, M. M. Abid, and J. Tang, “Application of the Bayesian model averaging in analyzing freeway traffic incident clearance time for emergency management,” *Journal of Advanced Transportation*, vol. 2021, Article ID 6671983, 9 pages, 2021.

[15] Institute of Studies for the Integration of Systems (ISIS), *Final Evaluation Report of the CIVITAS MODERN Project*, Institute of Studies for the Integration of Systems (ISIS), Rome, Italy, 2013.

[16] H. S. Levinson, J. S. Gluck, J. M. Barlow, R. W. Eck, and W. F. Hecker, “Driveway design practices, issues, and needs,” in *Proceedings of the 3rd Urban Street Symposium: Uptown, Downtown, or Small Town: Designing Urban Streets That Work*, pp. 1–21, Seattle, WA, USA, June 2007.

[17] Federal Highway Administration and Texas Transportation Institute, “Synthesis of Safety Research Related to Traffic Control and Roadway Elements,” Federal Highway Administration, Washington, D.C., USA, FHWA-TS-82-232, 1982.

[18] V. G. Stover and F. J. Koepke, *Transportation and Land Development*, Institute of Transportation Engineers, Washington, D.C., USA, 2002.

[19] J. L. Gattis, J. S. Gluck, J. M. Barlow, R. W. Eck, W. F. Hecker, and H. S. Levinson, *Geometric Design of Driveways*, Transportation Research Board, Washington, D.C., USA, NCHRP Project 15-35, 2009.

[20] A. Stokes, W. A. Sarasua, N. Huynh et al., *Safety Analysis of Driveway Characteristics along Major Urban Arterial Corridors in South Carolina*, Transportation Research Board, Washington, D.C., USA, No. 16-6766, 2016.

[21] M. A. Sultana, X. Qin, M. Chitturi, and D. A. Noyce, “Analysis of Safety Effects of Traffic, Geometric, and Access Parameters on Truck Arterial Corridors,” *Transportation Research Record: Journal of Transportation Research Board*, vol. 2404, 2014.

[22] M. Chowdhury, N. Huynh, S. M. Khan et al., *Operational and Economical Analysis of Access Management*, South Carolina Department of Transportation of Office of Materials and Research, Columbia, SC, USA, 2018.

[23] S. H. Richards, “Operational effects of driveway width and curb return radius,” *Transportation Research Record*, vol. 819, pp. 22–30, 1981.

[24] N. Gartner, C. J. Messer, and A. K. Rathi, *Traffic Flow Theory-A State-Of-The-Art Report: Revised Monograph on Traffic Flow Theory*, Federal Highway Administration, Washington, D.C., USA, 2002.

[25] X. Xin, N. Jia, S. Ma, and J. Mu, “Empirical and simulation study of traffic delay at un-signalized crosswalks due to conflicts between pedestrians and vehicles,” *Transportmetrica B: Transport Dynamics*, vol. 7, no. 1, pp. 637–656, 2018.

[26] X. Zhuo, N. Zhang, and Z. Qian, “Spacing calculation and selection on opposite vehicle access of large public building,” *Journal of Traffic and Transportation Engineering*, vol. 10, no. 4, pp. 71–78, 2010.

[27] Z. Qu, R. Luo, Y. Chen, N. Cao, X. Deng, and K. Wang, “Characteristics of right-turning vehicle trajectories at signalized intersection,” *Journal of Zhejiang University (Engineering Science)*, vol. 52, no. 2, pp. 341–351, 2018.

[28] CHELBI Engineering Consultants, Inc., *Specifications for Highway Safety Audit. People’s Republic of China Industry Standards JTG B05-2015*, China Communications Press Co., Ltd., Beijing, China, 2016.

[29] Ministry of Housing and Urban-Rural Development of the People’s Republic of China, “Code for Planning of Intersections on Urban Roads,” *National Standard of the People’s Republic of China GB50647-2011*, China Planning Press, Beijing, China, 2011.

[30] X. Zhuo, W. Shi, and Q. Shi, “Minimum spacing calculation for signalized intersections on the urban arterial,” *Journal of Transportation Systems Engineering and Information Technology*, vol. 14, no. 5, pp. 81–86, 2014.

[31] A. G. Ptv, *PTV Vissim 11 User Manual*, PTV, Karlsruhe, Germany, 2018.

[32] M. R. Parker and C. V. Zegeer, *Traffic Conflict Techniques for Safety and Operations - Observers Manual*, Federal Highway Administration, Washington D. C, USA, 1989.

[33] P. S. Bokare and A. K. Maurya, “Acceleration-deceleration behaviour of various vehicle types,” *Transportation Research Procedia*, vol. 25, pp. 4733–4749, 2017.

[34] H. Gao, W. Wang, B. Liu, and Y. Xiang, “Critical gap investigation at unsignalized intersections in China typical region,” *Journal of Southeast University (Natural Science Edition)*, vol. 30, no. 3, pp. 100–103, 2000.

[35] G. Yannis, E. Papadimitriou, and A. Theofilatos, “Pedestrian gap acceptance for mid-block street crossing,” *Transportation Planning and Technology*, vol. 36, no. 5, pp. 450–462, 2013.

[36] X. Zhuo, W. Zheng, Q. Wu, Y. Zhang, and L. Fu, “Green time optimization for artery traffic signal control system based on aggregation and dispersion,” *Journal of Guizhou University (Natural Sciences)*, vol. 38, no. 1, pp. 85–90+97, 2021.